ปฏิกิริยาไฮโดรจิเนชันแบบเลือกเกิดของอะเซทิลีนโดยตัวเร่งปฏิกิริยาแพลเลเดียม-ทอง และ แพลเลเดียม-คอปเปอร์ บนไทเทเนียที่เตรียมโดยการดูดซับแบบไฟฟ้าสถิตย์ที่แข็งแรงและการพอกพูนแบบไม่ใช้ไฟฟ้า

นางสาวนิศารัตน์ วิมลศุภกฤต

วิทยานิพนธ์นี้เป็นส่วนหนึ่งของการศึกษาตามหลักสูตรปริญญาวิศวกรรมศาสตรมหาบัณฑิต
สาขาวิชาวิศวกรรมเคมี ภาควิชาวิศวกรรมเคมี
คณะวิศวกรรมศาสตร์ จุฬาลงกรณ์มหาวิทยาลัย
ปีการศึกษา 2558

SELECTIVE HYDROGENATION OF ACETYLENE OVER TiO_2 SUPPORTED Pd-Au AND Pd-Cu CATALYSTS PREPARED BY STRONG ELECTROSTATIC ADSORPTION AND ELECTROLESS DEPOSITION

Miss Nisarat Wimonsupakit

A Thesis Submitted in Partial Fulfillment of the Requirements
for the Degree of Master of Engineering Program in Chemical Engineering
Department of Chemical Engineering
Faculty of Engineering
Chulalongkorn University
Academic Year 2015

Thesis Title	SELECTIVE HYDROGENATION OF ACETYLENE OVER TiO_2 SUPPORTED Pd-Au AND Pd-Cu CATALYSTS PREPARED BY STRONG ELECTROSTATIC ADSORPTION AND ELECTROLESS DEPOSITION
By	Miss Nisarat Wimonsupakit
Field of Study	Chemical Engineering
Thesis Advisor	Associate Professor Joongjai Panpranot, Ph.D.

Accepted by the Faculty of Engineering, Chulalongkorn University in Partial Fulfillment of the Requirements for the Master's Degree

.....Dean of the Faculty of Engineering
(Associate Professor Supot Teachavorasinskun, D.Eng.)

THESIS COMMITTEE

.....Chairman
(Associate ProfessorAnongnat Somwangthanaroj, Ph.D.)
.....Thesis Advisor
(Associate Professor Joongjai Panpranot, Ph.D.)
.....Examiner
(Assistant ProfessorSuphot Phatanasri, Ph.D.)
.....External Examiner
(Assistant ProfessorOkorn Mekasuwandumrong, D.Eng.)

นิศารัตน์ วิมลศุภกฤต : ปฏิกิริยาไฮโดรจิเนชันแบบเลือกเกิดของอะเซทิลีนโดยตัวเร่งปฏิกิริยาแพลเลเดียม-ทองและ แพลเลเดียม-คอปเปอร์ บนไทเทเนียที่เตรียมโดยการดูดซับแบบไฟฟ้าสถิตย์ที่แข็งแรงและการพอกพูนแบบไม่ใช้ไฟฟ้า (SELECTIVE HYDROGENATION OF ACETYLENE OVER TiO_2 SUPPORTED Pd-Au AND Pd-Cu CATALYSTS PREPARED BY STRONG ELECTROSTATIC ADSORPTION AND ELECTROLESS DEPOSITION) อ.ที่ปรึกษาวิทยานิพนธ์หลัก: รศ. ดร.จูงใจ ปั้นประณต, 75 หน้า.

ในงานวิจัยนี้ศึกษาการเติมทอง หรือ คอปเปอร์บนตัวเร่งปฏิกิริยาแพลเลเดียมบนตัวรองรับไทเทเนีย เพื่อปรับปรุงประสิทธิภาพของตัวเร่งปฏิกิริยาในปฏิกิริยาไฮโดรจิเนชันแบบเลือกเกิดของอะเซทิลีน ตัวเร่งปฏิกิริยาแพลเลเดียมบนตัวรองรับไทเทเนียใช้เตรียมโดยวิธีการดูดซับแบบไฟฟ้าสถิตย์ที่แข็งแรง ซึ่งสามารถได้การกระจายตัวของแพลเลเดียมสูง การเติมโลหะตัวที่สองบนตัวเร่งปฏิกิริยาแพลเลเดียมบนไทเทเนียทำโดยวิธีการพอกพูนแบบไม่ใช้ไฟฟ้าและเปรียบเทียบกับวิธีการเคลือบฝัง วิเคราะห์คุณลักษณะต่างๆ ของตัวเร่งปฏิกิริยาด้วยการไตรเตรตด้วยไฮโดเจนของออกซิเจนที่ปกคลุมบนพื้นผิวของแพลเลเดียม, การเลี้ยวเบนของรังสีเอ็กซ์, อินฟราเรดสเปกโตรสโกปีของการดูดซับคาร์บอนมอนอกไซด์, เอ็กซเรย์โฟโต้อิเล็กตรอนสเปกโตรสโกปี และ กล้องจุลทรรศน์อิเล็กตรอนแบบส่องผ่าน พบว่า แพลเลเดียมบนตัวรองรับไทเทเนียที่เตรียมด้วยวิธีการดูดซับแบบไฟฟ้าสถิตย์ที่แข็งแรง มีการกระจายตัวของแพเลเดียมสูงถึง 38 เปอร์เซนต์ ที่ประมาณ 1.29 เปอร์เซนต์โดยน้ำหนักของแพลเลเดียม การเติมโลหะตัวที่สองด้วยวิธีวิธีการพอกพูนแบบไม่ใช้ไฟฟ้า แสดงการเพิ่มขึ้นของการปกคลุมของโลหะตัวที่สองบนแพลเลเดียม ในขณะที่การเคลือบฝังมีการรวมตัวกันของโลหะตัวที่สองลงบนแพลเลเดียมและไทเทเนีย การกระจายตัวของกลุ่มแพลเลเดียมขนาดเล็กโดยวิธีการพอกพูนแบบไม่ใช้ไฟฟ้าส่งเสริมให้อะเซทิลีนเกิดการดูดซับแบบพันธะไพ ซึ่งสนับสนุนการไฮโดรจิเนชันไปเป็นเอทิลีน ตัวเร่งปฏิกิริยาคอปเปอร์บนแพลเลเดียมไทเทเนียที่เตรียมโดยการพอกพูนแบบไม่ใช้ไฟฟ้าแสดงการเลือกเกิดเป็นเอทิลีนและความว่องไวสูงกว่าตัวเร่งปฏิกิริยาทองบนแพลเลเดียมไทเทเนีย จากผลอินฟราเรดสเปกโตรสโกปีของการดูดซับคาร์บอนมอนอกไซด์ คาดว่าคอปเปอร์เลือกพอกพูนอย่างจำเพาะลงบนตำแหน่งโคออดิเนชันต่ำได้มากกว่าทอง ซึ่งช่วยยับยั้งการเกิดไฮโดรจิเนชันสมบูรณ์ของเอทิลีนเป็นอีเทน

ภาควิชา วิศวกรรมเคมี ลายมือชื่อนิสิต .....

สาขาวิชา วิศวกรรมเคมี ลายมือชื่อ อ.ที่ปรึกษาหลัก .....

ปีการศึกษา 2558

5770212221 : MAJOR CHEMICAL ENGINEERING

KEYWORDS: STRONG ELECTROSTATIC ADSORPTION / ELECTROLESS DEPOSITION / AU-PD BIMETALLIC CATALYSTS / CU-PD BIMETALLIC CATALYST

NISARAT WIMONSUPAKIT: SELECTIVE HYDROGENATION OF ACETYLENE OVER TiO_2 SUPPORTED Pd-Au AND Pd-Cu CATALYSTS PREPARED BY STRONG ELECTROSTATIC ADSORPTION AND ELECTROLESS DEPOSITION. ADVISOR: ASSOC. PROF. JOONGJAI PANPRANOT, Ph.D., 75 pp.

In the present work, the addition of Au or Cu on the performances of Pd/TiO_2 was investigation in the selective hydrogenation of acetylene for improve performance of catalyst. Pd was deposited on the titania support by the strong electrostatic adsorption (SEA) method, which can attain high dispersion of Pd. The addition of a second metal on Pd/TiO_2 was done by the electroless deposition (ED) method and compared with the incipient wetness impregnation (IM) method. The catalysts were characterized by hydrogen titration of oxygen-precovered on Pd, X-ray diffraction (XRD), Infrared spectroscopy of adsorbed CO (CO-IR), X-ray photoelectron spectroscopy (XPS), and transmission electron microscopy (TEM). The Pd/TiO_2 catalyst prepared by SEA showed highly dispersion of Pd at 38% at 1.29 wt.% Pd. The preparation by ED method showed incremental coverage of the second metal on Pd, while IM method had accumulation of second metal onto both Pd and TiO_2 support, the small ensembles of Pd sites found in ED samples promoted acetylene adsorption as **π**-bonded species that favored hydrogenation to ethylene. The $Cu\text{-}Pd/TiO_2$ catalysts prepared by ED showed higher ethylene selectivity and hydrogenation activity than the $Au\text{-}Pd/TiO_2$ catalysts. The results from CO-IR suggested that Cu selective deposited preferentially onto the low-coordination sites than Au which inhibited fully hydrogenation of ethylene to ethane.

Department: Chemical Engineering Student's Signature .....

Field of Study: Chemical Engineering Advisor's Signature .....

Academic Year: 2015

ACKNOWLEDGEMENTS

The author would like to express my greatest sincere and deepest appreciation to my advisor, Assoc. Prof. Dr. Joongjai Panpranot for her invaluable help and constant encouragement throughout the course of this research. I am most grateful for teaching and advice. I would not have achieved this fair and this thesis would not have been completed without all the support that I have always received from her.

I would like to thanks my committee member, Assoc. Prof. Dr. Anongnat Somwangthanaroj, Asst. Prof. Dr. Suphot Phatanasri, and Asst. Prof. Dr. Okorn Mekasuwandumrong, for letting my defense be an enjoyable moment, and for your brilliant comments and suggestion.

In addition, I would like to thank the financial support to this work under The Institutional Research Grant (The Thailand Research Fund), IRG 5780014, and Chulalongkorn University, Contract No. RES_57_411_21_076

Finally, I most gratefully acknowledge my parent and friends for all their support throughout the period of this research.

Nisarat Wimonsupakit

CONTENTS

Page

Page

Page

LIST OF TABLES

Page

LIST OF FIGURES

Page

CHAPTER 1
INTRODUCTION

1.1 Introduction

Ethylene is a high volume commodity that is important for polymer industry. It is used to produce chemical compounds such as ethylene oxide, polyethylene, and ethylene dichloride, which are precursors for many consumer products including surfactants, detergents, plastic bags, films and piping. Ethylene is produced by steam cracking of hydrocarbons and acetylene is a byproduct of this process. 0.5–2% of acetylene in ethylene is enough to poison the catalysts used to polymerize ethylene into polyethylene [1]. In order to eliminate acetylene from ethylene, two common techniques can be used: acetylene hydrogenation or separation of acetylene from the main stream. Since the separation method is expensive and dangerous, the most common industrial method of acetylene removal is acetylene hydrogenation [2].

Conventional, low Pd loading catalysts are used for this selective reaction in high concentration ethylene streams. Selectivity of acetylene to ethylene is the key objective, since over hydrogenation of acetylene to ethane results in a decrease in yield and must be recycled back to the ethane cracking unit [3]. Thus, over the years, bimetallic Pd catalysts have been developed for the selective hydrogenation of acetylene. Various additives, such as Ag, Ni, Cu, Au, Pb, Tl, Cr and K, have been reported to improve the performance of Pd catalysts, especially in achieving high selectivity for ethylene production [3-5]. Leviness et al.[6] reported the promotion of ethylene selectivity upon Cu addition, which they proposed to be due to a geometric effect. That is, the insertion of Cu into the Pd matrix decreases the number of multi-coordination sites of the Pd responsible for the dissociative adsorption of acetylene and suppresses the formation of beta phase Pd hydride as well; both are damaging to ethylene selectivity. On the other hand, Yunya et al. [3] reported the catalyst performances of Au-Pd/TiO_2 catalysts and suggested that at high coverages of Au on Pd, small ensembles of Pd sites were formed where acetylene is adsorbed as a π-bonded species that favored hydrogenation of acetylene to ethylene.

The Pd/SiO_2 catalysts with different transitional-metal oxide promoters (TiO_2, CeO_2) have been investigated by Moon et al. significant enhancement in the activity and ethylene selectivity in acetylene hydrogenation have been reported [7, 8]. The results have illustrated that the oxides on the Pd surface retarded the sintering of the dispersed Pd particles, suppressed the adsorption of ethylene in the multiply-bonded mode, and facilitated the desorption of ethylene produced by acetylene hydrogenation. TiO_2 gave better effects than those of CeO_2. It was reported that TiO_2 interacted strongly with the noble metal Pd, particularly after a reduction at high temperature like 500 °C. This phenomenum is referred to "the strong metal-support interaction" (SMSI) and has been observed on catalysts supported on reducible metal oxides, including CeO_2, $V2O_5$, and TiO_2. This interaction can remarkably change some catalysts activity and selectivity. In recent years, extensive researches using TiO_2 as support or promoter were investigated. For an SMSI between TiO_2 and Pd to arise, the catalyst must be reduced at high temperatures, e.g. 500 °C. However, the maximum temperature tolerable in most industrial reactors for acetylene hydrogenation is only about 300 °C, which is too low to induce the SMSI effect. Accordingly, improvements in ethylene selectivity by the use of added TiO_2 species is limited by industrial conditions. In this respect, new catalyst, which exhibits an SMSI phenomenon even after reduction at low temperatures, hopefully below 300 °C, would be highly desirable for industrial applications.

Strong electrostatic adsorption (SEA) is a special case of wet impregnation which the adsorption mechanism of metal ammine complexes over silica. It is reasonably well described as electrostatic interaction (physical adsorption) instead of ion exchange or chemical reaction. The SEA method appears to be a rational procedure for the cheap, simple, and scalable preparation of highly dispersed supported catalysts, even at relatively high metal loadings [9].

Several methods are available for preparing bimetallic composites, such as impregnation and subsequent reduction of two metal salts, galvanic displacement, and others. However, electroless deposition (ED) is a preparative methodology that provides a way to catalytically deposit in a controlled manner a second metal only on the surface of a pre-existing metallic surface (i.e., not on support). Thus, bimetallic

surface compositions can be more effectively controlled to permit more precise correlation of catalyst composition with performance using much lower amounts of the second metal [10].

In this research, the Pd/TiO_2 catalysts was prepared by SEA method and modified with Au and Cu, which was added using the ED method and tested in the selective hydrogenation of acetylene. The catalyst performances were correlated with the surface and structural properties of the Au-Pd and Cu-Pd/TiO_2 according to the characterization results from several characterization techniques.

1.2 Research objectives

To investigate the characteristics and catalytic properties of Pd/TiO_2 catalysts prepared by strong electrostatic adsorption and modified with Au and Cu prepared by electroless deposition method in selective hydrogenation of acetylene.

1.3 Research scope

1) Preparation of TiO_2 support Pd using strong electrostatic adsorption method

2) Preparation of Pd-based catalysts modified with Au and Cu using electroless deposition method and compared with those prepared by incipient wetness impregnation method.

3) Reaction study of catalyst sample in the selective hydrogenation of acetylene at 1 atm and 40 to 100 °C and GHSV of 2548 h^{-1}.

4) Characterization of the catalysts by the following techniques;

- Inductively coupled plasma optical emission spectrometry (ICP-OES)
- X-ray diffraction (XRD)
- Infrared spectroscopy of adsorbed CO (CO-IR)
- X-ray photoelectron Spectroscopy (XPS)
- Transmission electron microscopy (TEM)
- Hydrogen-oxygen titration

1.4 Research methodology

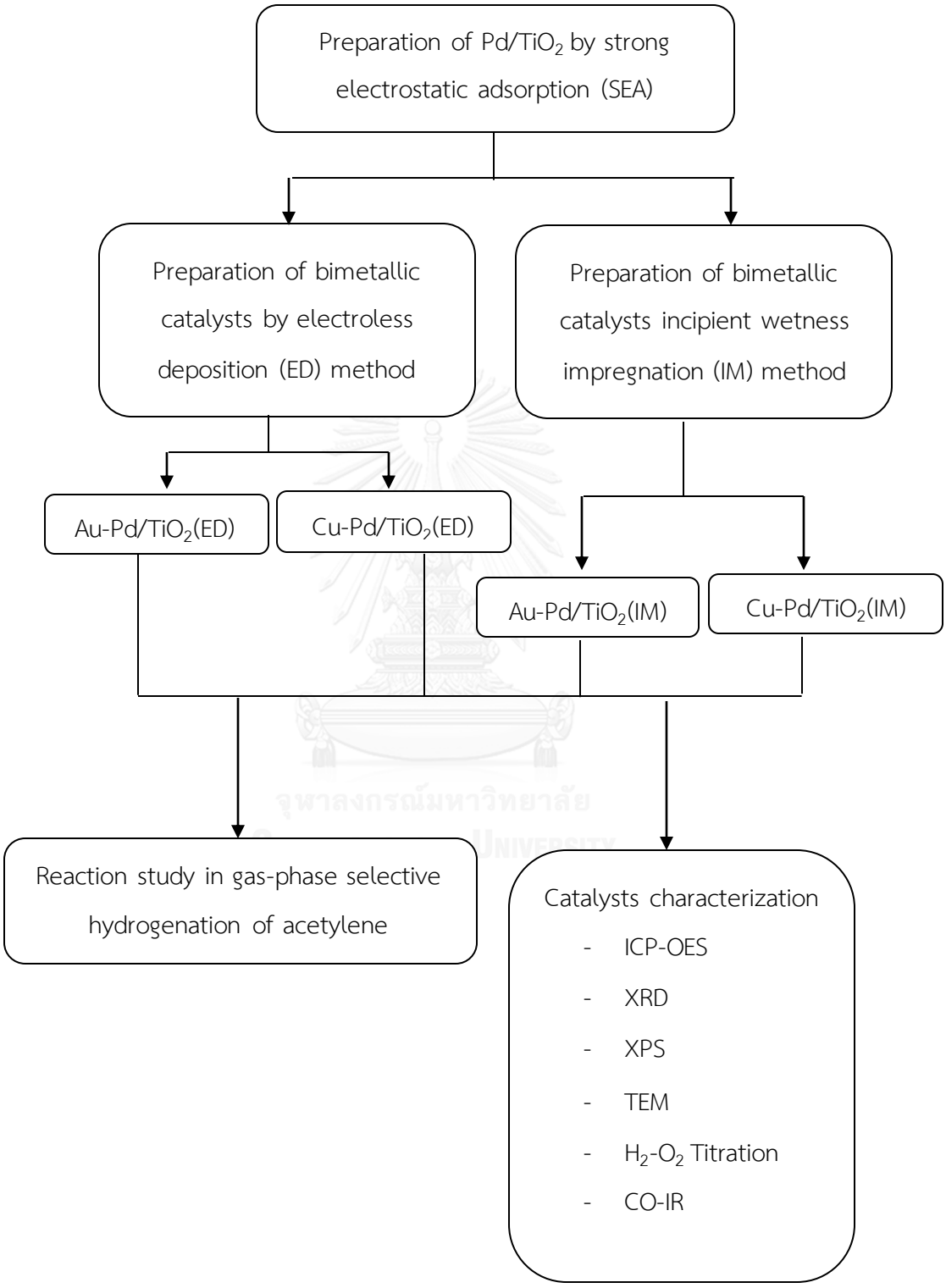

CHAPTER 2
THEORY AND LITERATURE REVIEWS

2.1. TiO_2 in general

TiO_2 has proven to be one of the promising n-type semiconductors due to its wide band gap (3.2 eV) under ultraviolet light [11]. Additionally, possessing high physical and chemical stability as well as the high refractive index makes this material widely researched [12]. Due to its electronic and optical properties, it can be utilized in several fields, such as solar cells, photocatalyst, sensors, and self-cleaning [13]. In electrochemistry, TiO_2 based materials play a key role due to their high conductivity and stability in alkaline and acid media. TiO_2 exists in three crystalline forms; anatase and rutile are the most common types, and the crystalline size of the rutile is always larger than the anatase phase. Brookite is the third structural form, an orthorhombic structure, which is rarely utilized, and is of no interest for most applications [14-17]. Rutile phase is the most thermally stable among the three phases. Brookite and anatase crystalline, above 600 °C, experience a phase transition and convert into the rutile phase [15, 16]. The anatase phase contains zigzag chains of octahedral molecules linked to each other, while the rutile consists of linear chains of opposite edge-shared octahedral structure [16-19]. Generally, the anatase-to-rutile phase transformation occurs between 600–700 °C, but, for certain applications, it is required that TiO_2 anatase be stable at 900 °C[18]. Generally, the anatase TiO_2 nanoparticles are stabilized by the addition of cations [19].

The synthesis techniques of TiO_2 usually require high temperatures to crystallize the amorphous material into one of the phases of TiO_2, such as brookite, anatase, and rutile, consequently leading to larger particles and typically nonporous materials [20-22]. Recently, low temperature synthesis methods resulted in crystalline TiO_2 with a higher degree of control over the formed polymorph and its intra- or interparticle porosities [19]. There are reports on the formation of crystalline nanoscale TiO_2 particle via solution based approach without thermal treatment with special focus on the resulting polymorphs, surface area, particle dimensions, and crystal morphology

[21]. There are exceptional emphases on the sol-gel method via glycosylated precursor and also the miniemulsion method [17-19].

TiO_2, due to its nontoxicity, long-term photo stability, and high effectiveness, has been widely utilized in mineralizing toxic and nonbiodegradable environmental contaminants. TiO_2 possesses good mechanical resistance and stabilities in acidic and oxidative environments. These properties make TiO_2 a prime candidate for heterogeneous catalyst support.

2.2 TiO_2 : As a support in heterogeneous metal catalysts.

Among different material candidates such as nitrides, perovskites, and carbides, TiO_2 based catalyst support materials are known to have excellent properties [23], due to TiO_2 nanoparticles high chemical and thermal stability. TiO_2 based catalyst supports have outstanding resistance towards corrosion in different electrolytic media. TiO_2 can be regarded as a support for heterogeneous catalysts which guarantees stability in electrochemical environment and commercial availability [24]. Meanwhile, strong interactions between the catalytic particles and mesoporous TiO_2 have been recorded, which, in the end, resulted in both improved catalytic stability and activity. TiO_2 as a catalyst support material also indicated a certain degree of proton conductivity, which may potentially enhance the regime of the triple phase boundary for catalytic reaction [23-25].

The study of metal nanoparticle on TiO_2 support is important in heterogeneous catalysis due to the size and nature of the interaction of a metal nanoparticle with TiO_2 support [24]. This interaction strongly influences the determination of catalytic activity and selectivity of the metal heterogeneous catalyst [25]. Reduction and oxidation at elevated temperature are compulsory steps in the preparation of metal supported TiO_2 heterogeneous catalyst [26, 27]. However, both treatments caused morphological changes to the dispersed metal nanoparticles from the sintering of TiO_2. Therefore, it is important that the optimal conditions for catalyst supported TiO_2 preparation be optimized, both in terms of pretreatment and activation [27, 28]. Besides, depending on the particular metal heterogeneous catalyst, different

morphological changes will result from metal-TiO_2 support interaction [29-31], such as sintering [29], alloy formation [31] encapsulation, and interdiffusion [30].

Among the TiO_2 modifications, anatase is frequently utilized as a catalyst support for metal heterogeneous catalyst due to its high specific surface area and strong interaction with metal nanoparticles [32, 33]. There are only a few studies reporting a rutile catalyst support which resulted in higher catalytic activity compared to anatase, such as the oxidation of toluene, xylene, and benzene over rutile-supported Cu catalyst. In comparison, rutile is preferred as a model support for particles of metals in surface science studies [34-36], due to its high crystal phase's thermodynamic stability. Furthermore, it is indicated that rutile and anatase differ noticeably in their ability of fixing particles of metals onto their respective surface [28, 36]; whereas the strong metal support interaction is normally shown on anatase, this effect is not as significant on rutile. Inopportunely, the thermodynamic stability of TiO_2 is comparatively low, and calcination would usually lead to the collapse of the porous structures [35]. Additionally, it is reported that calcination above 465 °C has always resulted in the phase transition from anatase to rutile [37]. The phase transition could be connected to the growth of crystal size, which results in a severe reduction in specific surface area [22]. Consequently, this should also influence the overall catalytic performance of metal heterogeneous catalysts.

2.3 Selective hydrogenation of acetylene over Pd-based catalysts

2.3.1 General information of selective hydrogenation of acetylene

The acetylene hydrogenation reaction scheme can be summarized as shown in **Figure. 2.1**. In general, there are two competing reaction pathways: hydrogenation to produce ethylene/ethane and oligomerisation leading to the formation of 1,3-butadiene and larger hydrocarbons. This later pathway is highly relevant given that oligomers are the precursor for the formation of 'green oil' which generally results in catalyst deactivation due to hydrocarbon accumulation on the catalyst surface. Therefore, in principle, the ideal catalyst for acetylene hydrogenation would avoid formation of oligomers. However, this seems extremely challenging with Pd based

catalysts and instead it is more realistic to look for catalysts which minimize the formation of 1,3-butadiene (small k_3 in **Figure 2.1**) or the buildup of larger oligomers which ultimately lead to deactivation (small k_4 in **Figure 2.1**) [38].

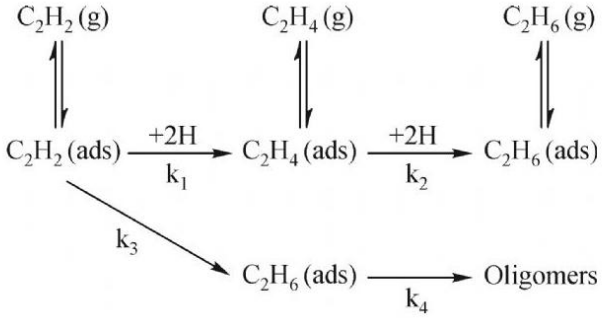

Figure 2.1 Reaction network for acetylene hydrogenation.

In order for a catalyst to selectively hydrogenate acetylene, it is imperative to maximize the rate of ethylene formation (large k_1 in **Figure 2.1**) whilst minimizing over-hydrogenation (k_2 in **Figure 2.1**). Recent literature suggests there are essentially two drivers for alkene selectivity thermodynamic selectivity and hindering hydride formation [39]. A catalyst which offers thermodynamic selectivity involves one where there is an energy barrier which hinders ethylene adsorption relative to acetylene adsorption meaning that over-hydrogenation is limited. This is not the main driver for palladium based catalysts but is the most controlling factor for moderate-high alkene selectivity over metals such as Cu, Ni, Au and Ag [40, 41].

To understand the factors that influence the selectivity in acetylene hydrogenation, it is important to consider the adsorption modes of acetylene on the catalyst surface. **Figure 2.2** shows identified adsorption modes of acetylene on a Pd surface, some in the presence of pre-adsorbed H. Both associative and dissociative acetylene adsorption can occur [3].

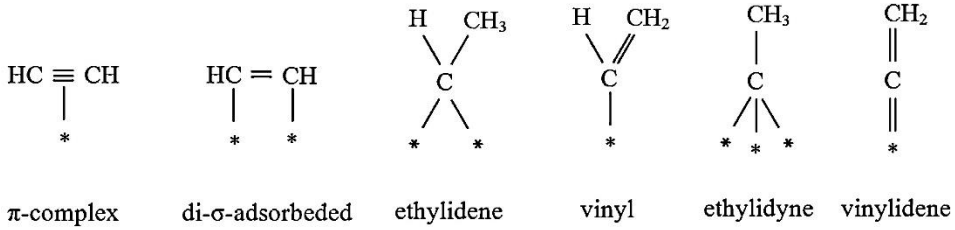

Figure 2.2 Adsorption modes of acetylene on Pd surface

A general mechanism shown in **Table 2.1** suggested that selectivity is controlled by the equilibrium between the two forms of adsorbed C_2H_3 (step 3 and step 4). The hydropolymerisation (formation of oligomer or "green oil") is consider to be a polymerisation of adsorbed acetylene, $H\,C^{*}=C^{*}H$, in which the free radical $-H\,C^{*}-C^{*}H$ is the initiator.

Table 2.1 General Mechanism of Catalytic Acetylene Hydrogenation

Step 1 : Adsorption	Acetylene is associatively adsorbed on the longer lattice spacing of the transition group metal, and that it reacts with a H_2 molecule (there being no independently adsorbed hydrogen on Ni) or	$H\,C^{*}=C^{*}H + H_2 \rightarrow H\,C^{*}=CH_2 + H^{*}$
	with an adsorbed H atom (on Pd or Pt).	$H\,C^{*}=C^{*}H + H^{*} \rightarrow H\,C^{*}=CH_2$
Step 2: Isomerisation	The adsorbed vinyl radical is thought to isomerise in part into a free radical form.	$-H\,C^{*}-C^{*}H_2$
Step 3: Hydrogenation to ethylene	The vinyl form hydrogenates to give ethylene which leaves the surface.	$H\,C^{*}=CH_2 + H^{*} \rightarrow CH_2=CH_2$
Step 4: Hydrogenation to ethane	The free radical form gives an adsorbed ethylene which can react with more hydrogen.	$-H\,C^{*}-C^{*}H_2 + H^{*} \rightarrow C^{*}H_2-C^{*}H_2$ $C^{*}H_2-C^{*}H_2 + H^{*} \rightarrow C^{*}H_2-CH_2$ $\rightarrow CH_3-CH_3$

2.3.2 Modification of Pd catalysts in the selective hydrogenation of acetylene

Acetylene impurities are usually removed by two methods, that is, adsorption with zeolite and conversion to ethylene by selective hydrogenation using Pd catalysts, the latter more commonly being used. Two factors are the keys to the assessment of this process. One is the ethylene selectivity, i.e., the fraction of ethylene produced by acetylene conversion, and the other is the catalyst lifetime which is limited by green oil deposition during the reaction. Various additives, such as Ag, Ni, Cu, Pb, Tl, Cr, and K, have been added to improve the performance of Pd catalysts, especially in achieving a high selectivity for ethylene production.

Table 2.2 Summary of the recent research on the Pd-based catalysts in acetylene hydrogenation.

Reference	Parameter studied and Characterization	Conclusions
E. W. Shin et al. (1998) [42]	Properties of Si-modified Pd catalyst. Catalysts : Pd/SiO_2, Pd/Al_2O_3, Si-Pd/SiO_2 and Si-Pd/Al_2O_3 Characterization : CO chemisorption, FTIR, acetylene-TPD, and XPS	The ethylene selectivity increased when the catalyst was modified with Si, while acetylene conversion was slightly lowered upon Si addition.
J. H. Kang et al. (2000) [7]	Transition-metal oxides added to Pd/SiO_2 improve significantly the activity and the ethylene selectivity. Catalysts : Pd-Ce/SiO_2, Pd-Nb/SiO_2, and Pd-Ti/SiO_2 Characterization : CO-IR, XPS, CO chemisorption, and acetylene-TPD,	The behavior of metal oxides in the catalyst is correlated well with their promotional effect on the catalyst performance. Ti oxide is found to have the most promotional effect

Reference	Parameter studied and Characterization	Conclusions
J. H. Kang et al. (2002) [8]	Preparation of Pd/SiO_2, Pd/TiO_2, and TiO_2-added Pd/SiO_2 catalysts, reduced them at different temperatures, and observed their performance in acetylene hydrogenation. Catalysts : Pd/SiO_2, Pd/TiO_2, and TiO_2-added Pd/SiO_2 Characterization : CO chemisorption, CO-IR, XPS, TEM, and ethylene-TPD	After reduction at 500 °C, the Pd surface was modified with the oxides, which migrated onto the Pd surface. The surface oxides retarded the sintering of the Pd particles and facilitated the desorption of ethylene from the Pd surface, which eventually promoted the ethylene selectivity and extended the lifetime of the catalysts.
W. J. Kim et al. (2004) [43]	Deactivation behavior of a TiO_2-added Pd catalyst. Catalysts : Pd/SiO_2 and TiO_2-added Pd/SiO_2 Characterization : H_2 chemisorption, CO-IR, XRD, and TGA	The average number of carbon atoms per green oil molecule was smaller for the TiO_2-added catalyst than for the Pd-only catalyst because multiply coordinated Pd sites were suppressed on the TiO_2-added catalyst.

Reference	Parameter studied and Characterization	Conclusions
K. Kontapakdee et al. (2007) [44]	Anatase and rutile TiO_2 were used for preparation of the TiO_2 supported Pd and Pd–Ag catalysts Catalysts : Pd/TiO_2-anatase, Pd/TiO_2-rutile, Pd-Ag/TiO_2-anatase, Pd-Ag/TiO_2-rutile Characterization : BET, XRD, ESR, and CO chemisorption	Pd/TiO_2-anatase exhibited higher acetylene conversion and ethylene selectivity than rutile TiO_2 supported ones. Ag promoted ethylene selectivity by blocking sites for over-hydrogenation of ethylene to ethane.
S. K. Kim et al. (2011) [4]	Cu-promoted catalysts was compared with Ag-promoted catalysts prepared by both the surface redox (SR) and the conventional impregnation method. Catalyst : Cu-Pd/Al_2O_3 and Ag-Pd/Al_2O_3 Characterization : ICP-AES, CO-IR, XPS, ethylene-TPD and STEM-EDS	The Cu-promoted catalysts prepared by SR showed higher ethylene selectivity and activity than Ag-promoted catalysts, particularly with small amounts of added promoter because Cu added by SR was deposited preferentially onto the low-coordination sites of Pd, which were detrimental to ethylene selectivity

Reference	Parameter studied and Characterization	Conclusions
Y. Zhang et al. (2014) [3]	The incremental surface coverages of Ag and Au on the Pd surface were prepared electroless deposition. Catalyst : Au-Pd/SiO_2 and Ag-Pd/SiO_2 Characterization : AAS and H_2-O_2 titration	At high coverages of Ag or Au on Pd, that result in small ensembles of Pd sites, acetylene is adsorbed as a π-bonded species that favors hydrogenation to ethylene. At low coverages, where ensemble sizes of contiguous Pd surface sites are much larger, acetylene is strongly adsorbed as a multi-σ-bonded species which preferentially forms ethane, lowering the selectivity to ethylene.
A. D. Benavidez et al. (2014) [1]	Effect of support of Pd nanoparticles with a narrow size distribution were deposited on three supports, carbon, alumina and magnesia. Catalyst : Pd/C, Pd/Al_2O_3 and Pd/MgO Characterization : BET, TEM-STEM, and EXAFS	The carbon-supported Pd yielded a higher selectivity to ethylene at 100% acetylene conversions (from acetylene/ethylene mixtures) when compared to the oxide-supported samples.

2.4 Strong electrostatic adsorption method

2.4.1 Theory

SEA is a special case of wet impregnation in which the final pH is targeted to the pH range in which the electrostatic interaction is strongest. One way strong interactions can be created is via the electrostatic adsorption mechanism illustrated in **Figure 2.3**. An oxide surface contains terminal hydroxyl groups that protonate or deprotonate, depending on the acidity of the impregnating solution. The pH at which the hydroxyl groups are neutral is termed the *point of zero charge* (PZC). Below this pH, the hydroxyl groups protonate and become positively charged, and the surface can adsorb anionic metal complexes such as platinum hexachloride $[PtCl_6]^{-2}$ (derived from chloroplatinic acid, CPA). Above the PZC, the hydroxyl groups deprotonate and become negatively charged, and cations such as platinum tetraammine $[(NH_3)_4Pt]^{+2}$ (PTA) can be strongly adsorbed [45].

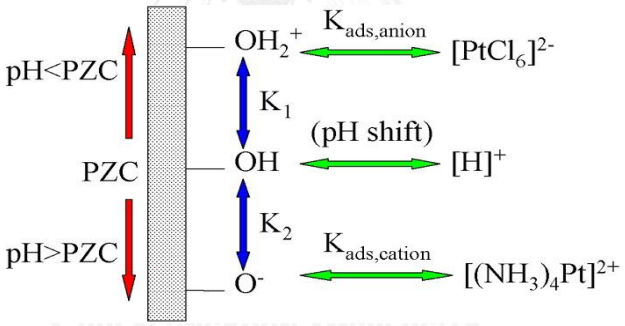

Figure 2.3 Mechanism of electrostatic adsorption.

The steps of the SEA approach for any particular metal/support system are then (a) the measurement of support PZC (which determines which charge of metal ion and which pH range to employ), (b) uptake-pH surveys to determine the pH of strongest interaction, and (c) tuning the reduction treatment to preserve high dispersion [45].

For a particular metal/oxide catalyst system, anionic or catonic metal complexes are chosen with respect to PZC of the oxide. For example, silica with an acidic PZC can accrue a strong negative charge as its surface hydroxyl group deprotonate and so the preferred metal complex is cationic. With their midrange PZC,

titania and alumina will adsorp anionic at low pH and cations at high pH. Anion adsorption would be preferred to basic neodymium hydroxide [46].

2.4.2 Synthesis of Pd-based catalysts by strong electrostatic adsorption method

It is very often the goal of the synthesis to create high metal surface area or, in other words, small metal crystallites anchored onto the support. The efficiency of metal utilization is commonly defined as dispersion, the fraction of metal atoms at the surface of a metal particle (and thus available to interact with adsorbing reaction intermediates) divided by the total number of metal atoms. Metal dispersion and crystallite size are inversely proportional; nanoparticles about 1 nm in diameter or smaller have dispersions of 100%, that is, every metal atom in the catalyst is available for reaction which can be prepared with SEA method.

Table 2.3 Summary of the recent research on the Pd-based catalysts by strong electrostatic adsorption method.

Reference	Metal and Characterizations	Studied	Conclusions
L. Jiao et al. (2008) [9]	Pd, Cu, Co, Ru and Ni on silica support Characterization : TPR, STEM, EDXS, and XPS	To determine the correlation between strong electrostatic interaction during impregnation and the high dispersion of reduced metals, a series of SiO_2-supported noble and base metal catalysts prepared by SEA was compared with the IWI method.	The SEA method appears to be a rational procedure for the cheap, simple, and scalable preparation of highly dispersed supported catalysts, even at relatively high metal loadings.

Reference	Metal and Characterizations	Studied	Conclusions
L. Jiao et al. (2008) [47]	Pt, Pd, Cu, Co, and Ru on SBA-15 Characterization : TPR, STEM, and EDXS	The catalyst synthesis method SEA was applied to mesoporous silica SBA-15.	- Low-temperature-reducing metals, such as Pt and Pd, form very well dispersed nanoparticles after reduction, with small standard deviation. - Co particles were larger, because the much higher temperature required for reduction of the adsorbed cobalt ammine complex led to metal sintering. - The SEA-prepared Co particles were still much smaller than the DI-prepared particles, which could be reduced at much lower temperature.

Reference	Metal and Characterizations	Studied	Conclusions
L. D'Souza et al. (2010) [48]	Pt/Co/C and Pd/Co/C Characterization : TPR, EDXS and EELS	The preparation of bimetallic electrocatalyst by SEA method.	Reduction at high temperature leads to homogeneously alloyed particles while lower temperature reduction leads to core-shell morphologies with a core of cobalt.

2.5 Electroless deposition method

2.5.1 Theory

The electroless deposition is a reducible metal salt (cation or anion) can be deposited on the catalytically active sites of a monometallic primary metal surface through a controlled chemical reaction with a liquid-phase reducing agent. The electroless deposition of a metal M, using a reducing agent R^{n-}, can be described with the following generic reaction:

$$M^{z+} + R^{n-} \longrightarrow M + R^{z-n} \qquad (1)$$

As shown by this reaction, the metallic ions M^{z+} will be reduced to metal M, while the reducing agent ions R^{n-} will be oxidized to R^{z-n} [49]. It is combination of two reaction occur simultaneously at the electrode surface. The anodic reaction is the oxidation of the reducing agent and the cathodic reaction is the reduction of the metal following in (2) and (3) [50].

$$R^{n-} \longrightarrow R^{z-n} + ze^{-} \qquad (3)$$

$$M^{z+} + ze^{-} \longrightarrow M \qquad (4)$$

The electroless deposition process shown in **Figure 2.4.** The aqueous reducing agent (RA) is catalytically activated at the surface of the primary metal (A) to produce

an active hydrogen species that reduces the aqueous secondary metal salt on the surface of the primary metal.

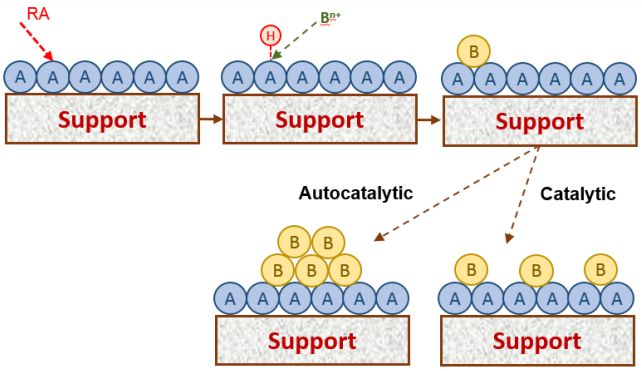

Figure 2.4 Principle for electroless deposition [60].

In the *autocatalytic* deposition there are various reducing agents (e.g., formaldehyde, hydrazine, hypophosphite, ascorbic acid, polyhydroxy alcohols, and hydrogen) that have been reported in the literature. The nature of the reducing agent can significantly influence the kinetics of electroless deposition as well as surface morphology and physicochemical properties of deposits [49].

2.5.2 Synthesis of Pd-based catalysts by electroless deposition method

ED is a catalytic or autocatalytic process for the selective deposition of reducible metal salts onto catalytically active sites through a controlled chemical reaction with a liquid-phase reducing agent that is catalyzed (typically at ambient conditions) by the pre-existing metal (catalysis) or the metal which is being deposited (autocatalysis). The successful application of ED requires a bath containing a reducible metal salt and an appropriate reducing agent that (1) is thermodynamically unstable, yet kinetically stable in the absence of a catalyst, (2) does not result in the electrostatic adsorption of the reducible metal salt on the catalyst support, and (3) gives controlled rates of catalytic deposition on the primary catalyst surface. These criteria require a balance of reactivity, stability, and ionic charge of the reducible metal salts.

Table 2.4 Summary of the recent research on the Pd-based catalysts prepared by electroless deposition method.

Reference	Metal and Characterizations	Studied	Conclusions
J. Rebelli et al. (2010) [10]	Au-Pd/SiO_2 Characterization : UV-Vis, AAS, FTIR, H_2-O_2 titration, STEM, EDS, and XPS	Synthesis and characterization of Au–Pd/SiO2 bimetallic catalysts prepared by electroless deposition for propylene hydrogenation	Au was deposited on all types of Pd surface sites (e.g., planes, steps, kinks, edges) in a non-discriminatory fashion, with a net electron transfer from Pd to Au. The catalysts were evaluated for propylene hydrogenation, revealing significantly enhanced turnover frequencies at elevated fractional coverage of Au on Pd.
J. Rebelli et al. (2011) [51]	Au-, Ag-, and Cu-Pd/SiO_2 Characterization : UV-Vis, AAS, FTIR, H_2-O_2 titration, and XPS	Optimization of the kinetic parameters of electroless deposition, including concentrations of the bis-cyano metal salt and reducing agent, solution pH, and temperature have been determined.	The deposition of Cu and Ag are selective towards Pd(1 1 1) sites, while Au deposits non-discriminately on all Pd sites.

Reference	Metal and Characterizations	Studied	Conclusions
Y. Zhang et al. (2014) [3]	Au- and Ag-Pd/SiO_2 Characterization : AAS and H_2-O_2 titration	The improvements in catalysts selectivity of acetylene to ethylene during acetylene hydrogenation and the roles of Ag and Au additives on the adsorption modes of acetylene on Pd.	Selectivity of acetylene to ethylene and TOF for acetylene conversion are enhanced at high coverages of Ag or Au on Pd, implying that the transition of adsorption mode of acetylene on Pd surface from strongly adsorbed ethylidyne on large Pd ensembles to weakly adsorbed, π-bonded species on small Pd ensembles, is responsible for selective conversion of acetylene to ethylene.
A. A. Rodriguez et al. (2014) [52]	Au–Pd/C Characterization : AAS , H_2-O_2 titration, XRD, and XPS	Liquid phase oxidation of glycerol under basic conditions was examined for a series of Au–Pd/C bimetallic catalysts prepared by electroless deposition.	Au can be systematically and controllably deposited on the Pd surface of a monometallic Pd/C catalyst to form catalysts with different surface compositions that provide a means to study Au–Pd bimetallic interactions for the oxidation of glycerol.

CHAPTER 3
EXPERIMENTAL

This chapter explains about the research methodology including the catalyst preparation, the experimental for acetylene hydrogenation reaction, and the characterization of catalysts, respectively.

3.1 Catalyst preparation

3.1.1 Preparation of Pd/TiO_2 using strong electrostatic adsorption method

The first step in the SEA method is to determine the PZC of the support. The titanium dioxide (surface area 50 m^2/g) was a commercial product from Sigma Aldrich. The TiO_2 was shaked in water solutions of various initial pH from 1 to 12 with HCl and NaOH for 1 h and after stabilization, the pH was measured again. The PZC value corresponds to a plateau in a pH_{final} *vs.* initial $pH_{initial}$ plot. For all measurements, the surface loading (SL), the total carbon surface in solution was fixed at 10^3 m^2/L. The PZC of the TiO_2, the pH_{final} value of the plateau equals 5.45.

Afterwards, the precursor adsorption curve *vs.* pH was determined. Since the PZC of the TiO_2 equals 5.45, the adsorption of $[Pd(NH_3)_4]^{2+}$ cations is favored for a pH higher than this value. The adsorption curve was measured by contacting 0.4 g of TiO_2 with 20 mL of 200 ppm of $Pd(NH_3)_4Cl_2$ aqueous solution, the pH of which was adjusted from 9 to 12 with NaOH. The mass of TiO_2 was chosen so as to fix the surface loading, *i.e.*, the total material surface area in solution, at 10^3 m^2/L. Contacted slurries were then placed on a rotary shaker for 1 h, after which the final pHs of these slurries were measured again. Two mL of the contacted slurries were withdrawn and filtered. The remaining concentration of Pd in the solution was determined by ICP-OES. Palladium uptakes from pH 9 to 12 were determined from the difference in Pd concentration between the pre-contacted and post-contacted solutions. The adsorption curve was then reported as the Pd surface density ($\mu molPd/m^2$) *vs.* the final pH of the solution. The adsorption curve shows that the maximum Pd uptake (1.1 $\mu molPd/m^2$, which corresponds to ~0.57 wt.%) is obtained for a final pH equal to 11.3 (initial pH = 11.82).

The metal surface density, Γ metal, is calculated at the concentration of metal adsorbed divided by the surface loading, that is,

$$\Gamma_{metal}(\mu mol/m^2) = \frac{(C_{metal,initial} - C_{metal,final})(\mu mol/L)}{SL(m^2/L)}$$

The SEA catalyst was then prepared by adjusting the final impregnation pH to this value. Ten gram of TiO_2 was shaked in 0.5 L of $Pd(NH_3)_4Cl_2$ solution (200 ppm), the pH of which was adjusted to 11.3 with NaOH prior to TiO_2. Therefore, the surface loading (SL) was again fixed at 10^3 m^2/L. After 1 h under rotary shaker at ambient temperature, the slurry was filtrated, measured remain concentration of Pd and the recovered solid was dried in vacuum filter for 12 h. The catalyst obtained was then reduced under flowing H_2 at 200 °C for 2 h.

Table 3.1 Chemical composition use for prepared Pd/TiO_2 by strong electrostatic adsorption.

Chemicals	Formula	Supplier
Titanium dioxide, Anatase, 99%	TiO_2	Aldrich
Tetraamminepalladium(II) chloride monohydrate	$Pd(NH_3)_4Cl_2 \cdot H_2O$	Aldrich
Sodium hedroxide	NaOH	Aldrich
Hydrochloric Acid, 37%	HCl	RCI Labscan

3.1.2 Preparation of Au- and Cu-Pd/TiO_2 using electroless deposition method

The 1.28 wt.% Pd/TiO_2 catalyst from SEA was used for preparation of Au and Cu on Pd/TiO_2 by electroless deposition method. The palladium dispersion of 37.86% was determined using the chemisorption method described below in the characterization section; dispersion of 37.86% for 1.28 wt.% Pd corresponds to 2.76×10^{19} surface Pd sites/g cat. The Au-Pd/TiO_2 and Cu-Pd/TiO_2 bimetallic catalysts were

synthesized using cyanide metal precursors. Metal salt/reducing agent molar ratios of 1:10 were used with hydrazine as the reducing agent for Au deposition as well as dimethylamineborane (DMAB) for Cu deposition. Initial concentrations of the metal salts were selected based on theoretical coverage of Au on Pd, assuming monolayer deposition and 1:1 surface stoichiometry of metal deposited on Pd.

Typically, electroless bath concentration of Au and Cu were varied, depending on the targeted weight loadings of the second metals. The deposition of Au was carried out at room temperature, while ED of Cu was conducted at 40 °C. All baths were vigorously stirred to minimize any possible external mass transfer limitations and the solution pH was maintained at 9±0.5 by careful addition of concentrated NaOH solution. Small aliquots of ED solution (<2 ml) were collected and filtered using a syringe filter at various time intervals of deposition to monitor the concentrations of Au and Cu salts remaining in the bath during deposition. After the completion of ED (60 min), the slurry was filtered and washed repeatedly until all the remaining water soluble ligands (i.e., residual $Au(CN)^{2-}$, $Cu(CN)^{2-}$, CN^{-}, and Cl^{-}) were removed. The wet sample cakes were dried under vacuum at room temperature and stored at ambient conditions. Thus, a series of each of the bimetallic catalysts with incremental Au and Cu weight loadings and surface coverages on Pd was synthesized.

Table 3.2 Chemical composition use for prepared Au- and Cu-Pd/TiO_2 by electroless deposition.

Chemicals	Formula	Supplier
Potassium dicyanoaurate(I), 98%	$KAu(CN)_2$	Aldrich
Hydrazine solution, 35 wt.% in H_2O	N_2H_4	Aldrich
Potassium dicyanocuprate	$KCu(CN)_2$	STREM
Borane dimethylamine, 97%	$(CH_3)_2NH{\cdot}BH_3$	Aldrich
Sodium hedroxide	NaOH	Aldrich

3.1.3 Preparation of Au- and Cu-Pd/TiO_2 using with incipient wetness impregnation method

The 1.28 wt.% Pd/TiO_2 catalyst from SEA was used for preparation of Au and Cu on Pd/TiO_2 by incipient wetness impregnation method. Pd/TiO_2 catalyst were impregnated with an aqueous solution of gold (III) chloride trihydrate and Copper(II) nitrate trihydrate for Au-Pd/TiO_2 and Cu-Pd/TiO_2, respectively. The impregnated catalysts were left to stand for 6 hours to assure adequate distribution of metal complex. The catalysts was subsequently dried at 100°C in air overnight. The dried impregnation catalysts were calcined under nitrogen with heating rate was at 10°C/min until the temperature reached 350°C for Au and 450°C for Cu. Then flowing air was switched into the reactor to replace nitrogen and the temperature was hold for 3 hour. The calcined sample was finally cooled down and stored in a glass bottom for later use.

Table 3.3 Chemical composition use for prepared Au- and Cu-Pd/TiO_2 by with incipient wetness impregnation method.

Chemicals	Formula	Supplier
Gold(III) chloride trihydrate	$HAuCl_4 \cdot 3H_2O$	Aldrich
Copper(II) nitrate trihydrate	$Cu(NO_3)_2 \cdot 3H_2O$	Aldrich

3.2 Catalyst characterization

All catalysts were characterized by several techniques as follows:

3.2.1 ICP-OES

The concentration of metal in preparation of catalysts by strong electrostatic adsorption and electroless deposition method were measured by ICP-OES, using the Optima 2100 DV spectrometer.

3.2.2 XRD

The XRD was used determined XRD patterns of all the supports and all the catalysts by using the SIEMENS D5000 x-ray diffractometer connected with a computer with Diffract ZT version 3.3 programs for fully control of the XRD analyzer. The experiments were carried out by using CuK_{α} radiation with Ni filter in the 2θ range of 20° to 80° and resolution 0.04°.

3.2.3 XPS

The XPS spectra, the blinding energy, full width at half maximum (FWHM) and the composition of the all catalysts on the surface layer of the catalysts were performed by using the Kratos Amicus x-ray photoelectron spectroscopy. The experiment was operated with the x-ray source at 20 mA and 12 kV (240 W), the resolution at 0.1 eV/step and the pass energy of the analyzer was set at 75 eV under pressure approximately $1x10^{-6}$ Pa. For calibration, the blinding energy was referenced to C 1s line at 285.0 eV. The C 1s line was taken as an internal standard at 285.0 eV. The blinding energy of O 1s, Ti 2p, Pd 3d, Au 4f, and Cu 2p are determined.

3.2.4 CO-IR

The CO adsorbed on the metal surface were measured using FTIR spectrometer (Bruker) with a liquid nitrogen-cooled MCT detector. In these measurements, pellets of 1.5 cm diameter were prepared by pressing ~0.05 g of sample at 6000 lb force and then placed in a temperature-controlled flow cell. He gas was introduced into sample cell in order to remove the remain air. The sample were reduced in H_2 for 1 h at 200 °C, cooled to 30 °C with He gas. For each pellet, a background spectrum in flow He was taken and subtracted from all subsequent spectra. The pellet was exposed to CO for 15 min and then was purge with He gas to remove gas phase and physisorbed CO. The FTIR spectra were recorded in the 400-4000 cm^{-1} range at a wavenumber resolution of 4 cm^{-1} and 150 scans.

3.2.5 TEM

The palladium oxide particle sized and distribution of palladium on titanium dioxide were observed using JEOL-JEM 2001 CX transmission electron microscope operated at 100 kV.

3.2.6 Hydrogen-Oxygen Titration

Chemisorption using hydrogen pulse titration of oxygen-precovered Pd was performed using a Micromeritics ChemiSorb 2750 automated system attached with ChemiSoft TPx software. Prior to titration, approximately 0.05 g sample was reduced in flowing pure H_2 at 200 °C for 2 h, then exposed to 100% Ar flow for 1 h at 200 °C to remove chemisorbed hydrogen from the metal surface. After cooling to 40 °C in flowing Ar, the sample was exposed to 1% O_2/balance He for 30 min to saturate the Pd surface with adsorbed atomic oxygen. Following exposure to 100% Ar for 30 min to remove residual O_2, the sample was ready for pulse flow H_2 titration. At room temperature the adsorbed atomic oxygen reacts rapidly with the pure H_2 pulse to form H_2O and replace the adsorbed oxygen atom with atomic hydrogen. Hydrogen consumption was quantitatively determined by means of a high sensitivity thermal conductivity detector (TCD) below the sample cell. Hydrogen pulses were continued until no further uptake of H_2 was observed. Hydrogen titration of O-precovered Pd was used rather than H_2 chemisorption because of problems associated with formation of bulk β-palladium hydrides; likewise, chemisorption of CO was not used due to uncertainties of CO/surface Pd stoichiometry. At the timescale used for H_2 pulse titrations, H_2 rapidly reacts with adsorbed O atoms to form H_2O and to cover the vacant Pd site with atomic H without formation of b-palladium hydride. For each Pd atom, 1.5 H_2 molecules are consumed. Since Au and Cu are inactive for hydrogen–oxygen titration, the concentration of Pd surface sites that were covered by Au or Cu metals can be determined by subtracting the Pd surface site concentration of the bimetallic catalysts from the total number of surface Pd sites for the monometallic Pd/TiO_2 catalyst.

3.3 Catalytic reaction in hydrogenation of acetylene

The catalytic performance for the selective hydrogenation of acetylene was measured at different temperatures. Feed gas composed of 1.5%C_2H_2, 1.7%H_2, and balance C_2H_4. The reaction products and feed composition were analyzed by a gas chromatograph equipped FID (SHIMADZU FID GC 8APF, Carbosieve column S-II) detector for separating C_2H_2, C_2H_4, and C_2H_6 and a gas chromatograph equipped TCD (SHIMADZU TCD GC 8APT, Molecular sieve 5A) detector for analyzing H_2. The operating conditions for each instrument are summarized in **Table 3.4**.

Table 3.4 Operating conditions of gas chromatograph for selective hydrogenation of acetylene.

Gas chromatograph	SHIMADZU GC 8APF	SHIMADZU GC 8APT
Detector	FID	TCD
Packed column	Carbosieve column S-II	Molecular sieve 5A
Carrier gas	N_2	Ar
Carrier gas flow rate (ml/min	40-60	40-60
Injector temperature (°C)	180	80
Detector temperature (°C)	180	80
Initial column temperature (°C)	100	50
Programmed rate (°C/min)	10	-
Final column temperature (°C)	160	50
Current (mA)	-	70
Analyzed gas	C_2H_2, C_2H_4, C_2H_6	H_2

Catalyst 0.15 g was packed in a pyrex tubular downflow reactor of 10 mm in diameter. Reactor was placed into the furnace and purge with argon for remove remaining air. Prior to the start of each experimental run, the catalyst was reduced with hydrogen by heating from room temperature to 150 ℃ for 2 h at a heating rate of 10 ℃/min. Then the reactor was purged with argon and cooled down to the reaction temperature 40℃. The reactant gases was introduce at temperature from 40℃ to 100℃ and 1 atm and sampling was taken every 1 h, which was approximately within 1 h.

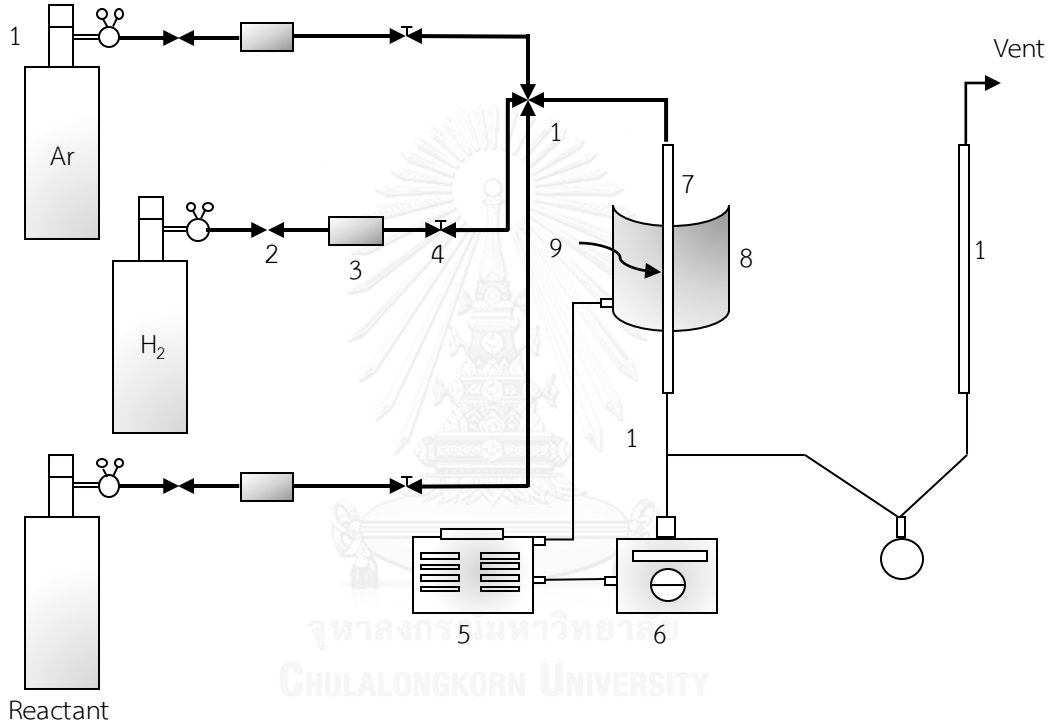

Figure 3.1 A schematic of acetylene hydrogenation system

1. Pressure regulator
2. On-off value
3. Gas filter
4. Needle value
5. Variable voltage transformer
6. Temperature controller
7. Reactor
8. Furnace
9. Catalyst bed
10. Thermocouple
11. 4-way joint
12. Bubble flow meter

CHAPTER 4
REULTS AND DISCUSSION

This chapter describes the results with a discussion about Pd based monometallic and bimetallic catalysts in the selective hydrogenation of acetylene. The results and discussion are divided in three sections. The first section describes the characterization of Pd/TiO_2 catalyst prepared by strong electrostatic adsorption. The second section describes the characterization and catalytic properties of the bimetallic $Au\text{-}Pd/TiO_2$ and $Cu\text{-}Pd/TiO_2$ prepared by electroless deposition method compared with those prepared by the incipient wetness impregnation method. The last section describes the catalytic performances of monometallic and bimetallic catalysts in the selective acetylene hydrogenation.

4.1 Properties of Pd/TiO_2 catalyst prepared by SEA.

4.1.1 ICP-OES

Figure 4.1 displays the pH shift of TiO_2 at 1000 m^2/L without metal in solution at a contact time of 1 h. The plateau of pH shift plot corresponds to the PCZ of TiO_2 support. From this profile, it can be seen that TiO_2 has PCZ values around 5.4. In adsorption surveys, the initial pH values were adjusted more than PCZ values in the range of 6-12 for the adsorption of palladium tetraammine precursor over TiO_2. The adsorption curve of Pd over TiO_2 at 1000 m^2/L with the revised physical adsorption is shown in **Figure 4.2**, the maximum Pd uptake was observed in the pH range of 10-11.

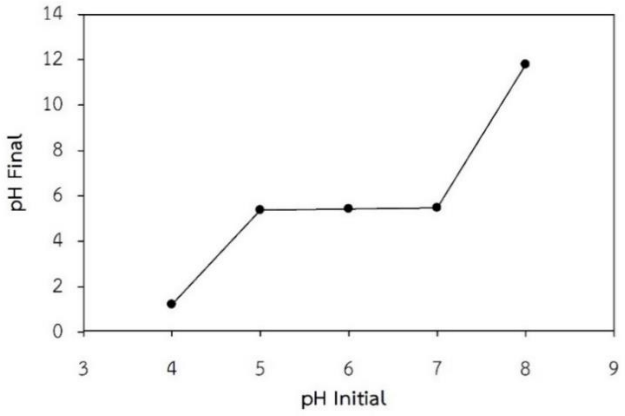

Figure 4.1 The point of zero chart of TiO_2.

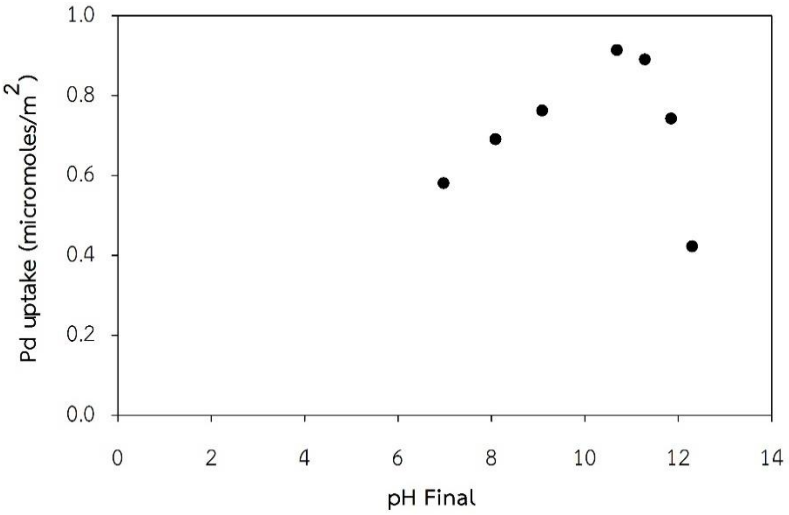

Figure 4. 2 The uptake of Pd on TiO_2 support as a function of pH.

4.1.2 XRD

The XRD patterns of TiO_2 support and 1.29%Pd/TiO_2 (SEA) reduced with H_2 at 200 °C for 2 h are shown in **Figure 4.3**. The measurement was carried out at the diffraction angles (2θ) between 20° and 80°. The diffraction peak of TiO_2 were observed at the main characteristic peaks positioned at 2θ = 25°, 37°, 48°, 54°, 56°, 62°, 69°, 70° and 75°. There were no changes in crystalline phase composition of the TiO_2 after palladium loading. The XRD peaks corresponding to Pd species such as PdO were not observed at 2θ = 33.8° due to very small crystallite size or low amount of Pd loading. The crystallite size of both TiO_2 for pure support and Pd/TiO_2 was similar around 15-17 nm from Sherrer equation.

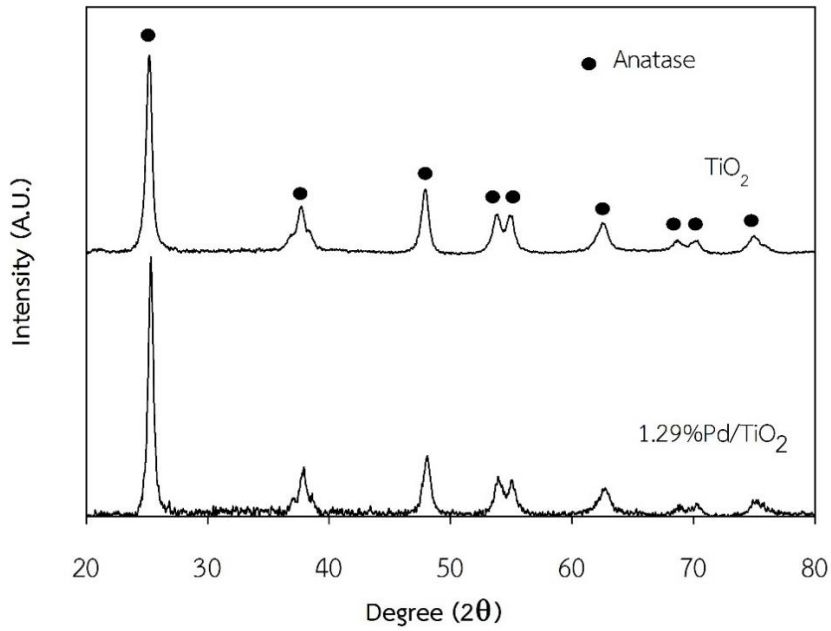

Figure 4.3 The XRD patterns of the TiO_2 and Pd/TiO_2.

4.2 Properties of Au-Pd/TiO_2 and Cu-Pd/TiO_2 catalysts prepared by electroless deposition method and incipient wetness impregnation method.

4.2.1 ICP-OES

The series of Au- and Cu-Pd/TiO_2 were prepared by increasing of Au and Cu coverages on the Pd surface. For initial step of electroless deposition, the monometallic (Pd) catalyst surface activates the reducing agent. And then the second metal considered here, Au has a higher oxidation capability compared to Pd, which should result in the catalytic deposition of Au on Pd surface being favored at submonolayer coverages of Au. At latter stages of electroless deposition, the Pd surface became more coverage by Au, both catalytic and autocatalytic will likely occur [10]. Likewise, Cu occurred as well. Approximately 1 g of Au-Pd/TiO_2 and Cu-Pd/TiO_2 bimetallic catalysts prepared by varying initial concentration of second metal salt. The deposition profiles are summarized in **Figure 4.4** and **Figure 4.5** for Au-Pd/TiO_2 and Cu-Pd/TiO_2, respectively.

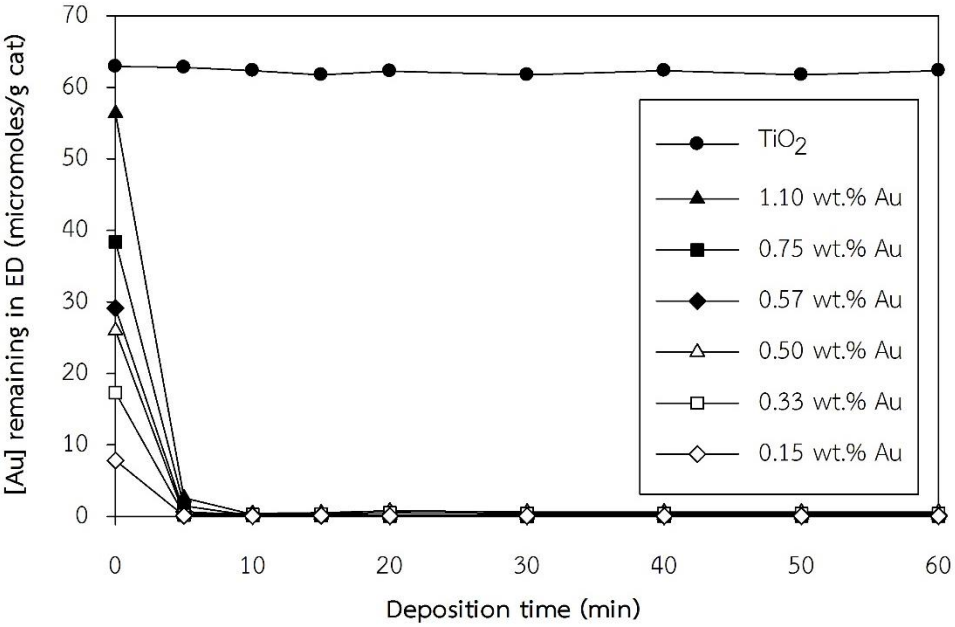

Figure 4.4 Au deposition profile for the synthesis of Au-Pd/TiO_2

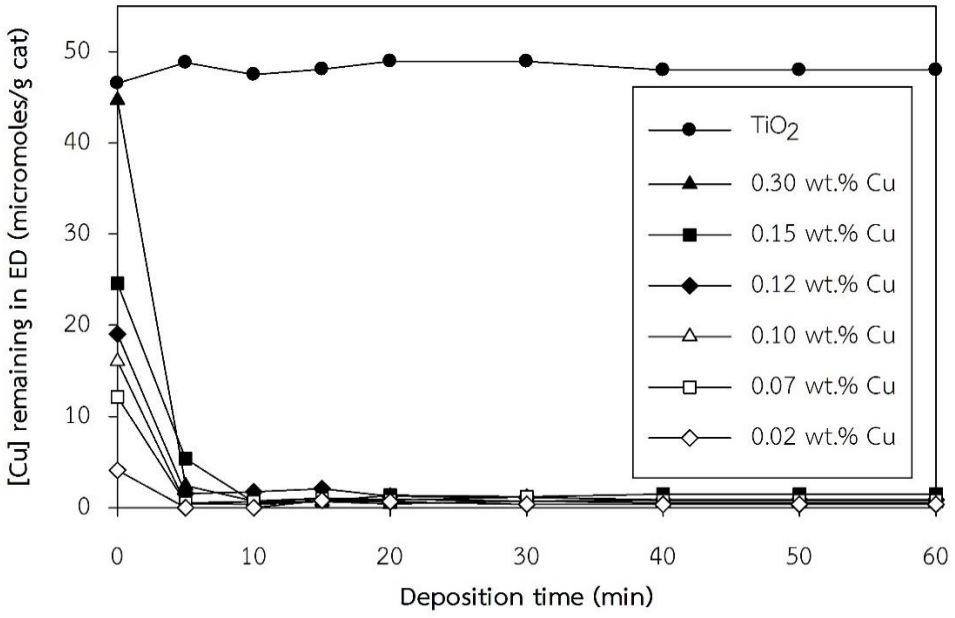

Figure 4.5 Cu deposition profile for the synthesis of Cu-Pd/TiO_2

4.2.2 XRD

The XRD patterns of Au- and Cu-Pd/TiO_2 bimetallic catalysts, which prepared by electroless deposition method are shown in **Figure 4.6** and **Figure 4.7**. The diffraction peak of TiO_2 were observed at the main characteristic peaks positioned at 2θ = 25°, 37°, 48°, 54°, 56°, 62°, 69°, 70° and 75°. There were no changes in crystalline phase composition of the TiO_2 after Au or Cu loading. The Au- and Cu-Pd/TiO_2 bimetallic catalysts were prepared by incipient wetness impregnation method at same percent weight of second metal. The XRD patterns were investigated after calcined under air at 350 °C and 400 °C for Au-Pd/TiO_2 and Cu-Pd/TiO_2, respectively. The same characteristic peak of pure anatase phase was found as well as Pd/TiO_2 and bimetallic prepared by elecroless deposition method. Likewise, both method for addition of second had no effect on crystallite size of TiO_2, which had crystallite size around 15-17 nm.

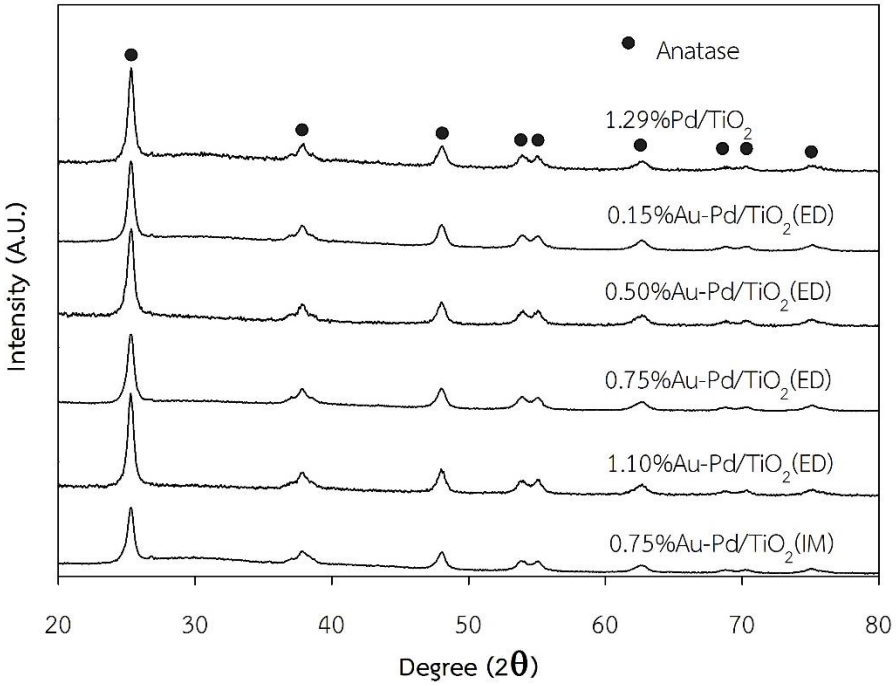

Figure 4.6 The XRD patterns of the Pd/TiO_2 and Au-Pd/TiO_2

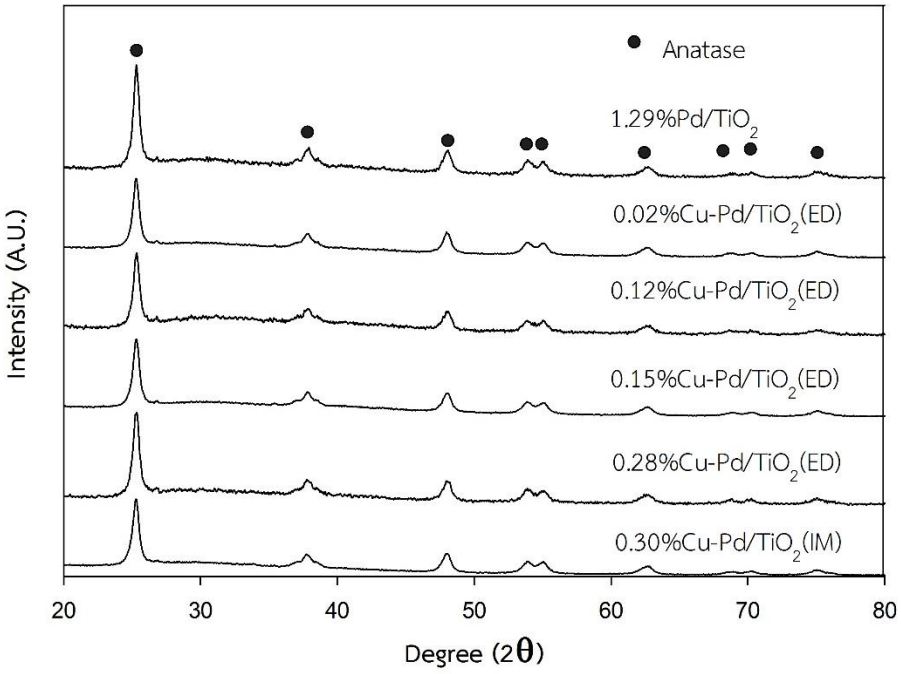

Figure 4.7 The XRD patterns of the Pd/TiO_2 and $Cu\text{-}Pd/TiO_2$

4.2.3 Hydrogen-Oxygen Titration

The Pd surface site concentration for Pd/TiO_2 and all the bimetallic catalysts were determined by chemisorption using the preferred method of hydrogen of oxygen-precovered Pd sites [53]. Because Au and Cu are inactive for hydrogen titration of oxygen-precovered surface, the Au or Cu coverage on Pd surface can be calculated by subtracting their values from the total number of Pd sites of monometallic Pd/TiO_2 catalyst. In **Table 4.1**, the dispersion of Pd decreased with increase Au or Cu coverage for preparation of electroless deposition method. The decreasing is due to blockage of surface Pd site by the electrolessly deposited second metal or Pd leaching by free CN^- ligands or gelation of the titania support causing erosion of Pd particles. ICP analysis of the electroless deposition bath and filtrates analyzed before, during, and after exposure of Pd/TiO_2 to pH 9 solution detected no Pd content. Hence, the decrease in Pd surface sites with increase of Au or Cu is due to electroless deposition of Au or Cu metal on surface Pd sites.

Table 4.1 Chemisorption results using hydrogen of oxygen-precovered on Pd sites. The theoretical coverage refers to theoretical monodisperse layer of Au or Cu on Pd and actual coverage refers to Au or Cu coverage determined from chemisorption.

Sample	Dispersion (%)	Theoretical coverage (ML)	Actual coverage
1.286%Pd/TiO_2	37.9	-	-
0.15%Au-Pd/TiO_2(ED)	32.5	0.17	0.14
0.33%Au-Pd/TiO_2(ED)	32.2	0.37	0.15
0.50%Au-Pd/TiO_2(ED)	26.3	0.55	0.31
0.57%Au-Pd/TiO_2(ED)	23.5	0.63	0.38
0.75%Au-Pd/TiO_2(ED)	17.1	0.83	0.55
1.10%Au-Pd/TiO_2(ED)	15.6	1.22	0.59
0.75%Au-Pd/TiO_2(IM)	32.3	0.83	0.15
0.02%Cu-Pd/TiO_2(ED)	35.6	0.07	0.06
0.07%Cu-Pd/TiO_2(ED)	34.5	0.24	0.09
0.10%Cu-Pd/TiO_2(ED)	26.5	0.34	0.30
0.12%Cu-Pd/TiO_2(ED)	23.9	0.41	0.37
0.15%Cu-Pd/TiO_2(ED)	18.9	0.52	0.50
0.28%Cu-Pd/TiO_2(ED)	17.4	0.96	0.54
0.30%Cu-Pd/TiO_2(IM)	28.7	1.03	0.24

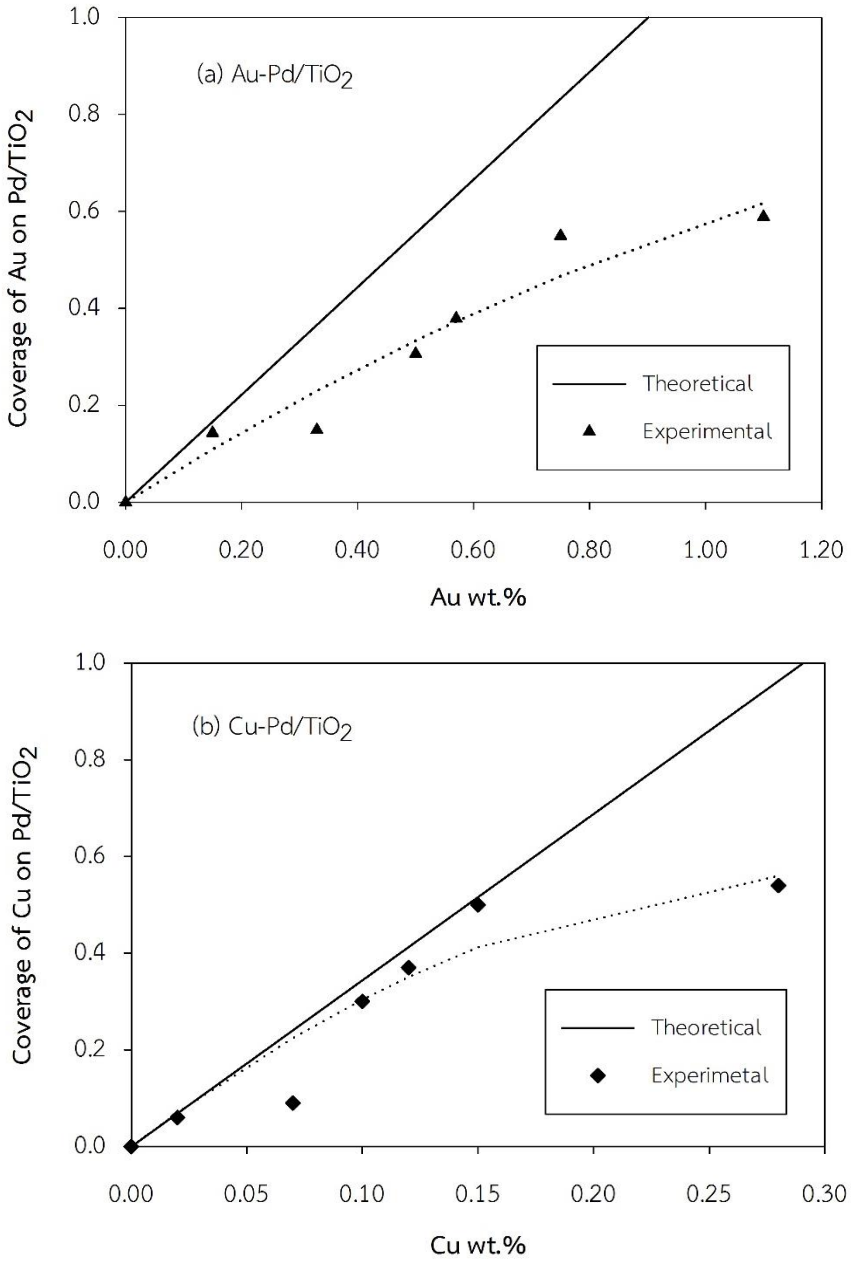

Figure 4.8 Actual coverage of Au or Cu on Pd/TiO_2 as a function of weight of Au or Cu deposition for (a) Au-Pd/TiO_2 and (b) Cu/Pd/TiO_2. The solid line is the theoretical coverage of Au or Cu metal on Pd surface at a 1:1 deposition stoichiometry.

The deviation of exposed Pd sites from the theoretical curves for monodisperse coverages of Au/Pd or Cu/Pd at a 1:1 deposition stoichiometry indicates that autocatalytic deposition occurs for bimetallic catalyst. In **Figure 4.8**, transition from catalytic deposition to autocatalytic deposition occurs at approximately 0.2 coverage

of Au and 0.5 coverage of Cu metal deposition on Pd. 0.15 wt.% Au and 0.15 wt.% Cu are required to give monodisperse coverage on Pd. Below this level of deposition, catalytic deposition predominates while both catalytic and autocatalytic deposition occur at above this point.

Comparing the methods for deposition of a second metal on Pd/TiO_2, the electroless deposition method is more effective in coverage of Au or Cu on Pd sites more than the incipient wetness impregnation method at a similar weight of Au or Cu.

4.2.4 CO-IR

To determine whether site-specific deposition of Au or Cu on Pd surface occurs, FTIR spectroscopy of CO adsorbed on Pd sites was conducted at 30 °C. FTIR spectra for various Au and Cu loadings on Pd/TiO_2 which prepared by electroless deposition and incipient wetness impregnation method are shown in **Figure 4.9** and **Figure 4.10**, respectively. The CO stretching bands were observed in both 2000-2100 cm^{-1} and 1800-2000 cm^{-1} region, due to linearly and multiply-coordinated CO on Pd sites, respectively [54]. The linear region was further deconvoluted in to two peaks centered at 2077-2100 cm^{-1} and 2068-2074 cm^{-1}, which were attributed to linearly bonded CO molecules on defect of low coordination sites such as corners, steps and kinks of Pd(111) and Pd(100) surfaces, respectively [51]. The region between 1800 and 2000 cm^{-1} contains several overlapping features, which was resolved into peaks at 1978, 1938, 1876 and 1812 cm^{-1}. The peak at 1978 and 1938 cm^{-1} can be assigned to twofold, bridged CO species on low index planes such as Pd(110) and Pd(100), respectively [54-56]. The peak at 1876 and 1812 cm^{-1} are consistent with CO adsorption on three-fold hollow sites on Pd(111) surfaces [54, 57]. However, for CO adsorption on $Cu-Pd/TiO_2$ catalysts, there was a moderately strong peak at 2130-2110 cm^{-1} which could be assigned to CO adsorption on Cu and/or Cu^+ sites [51]. All relevant band assignments are summarized in **Table 4.2**.

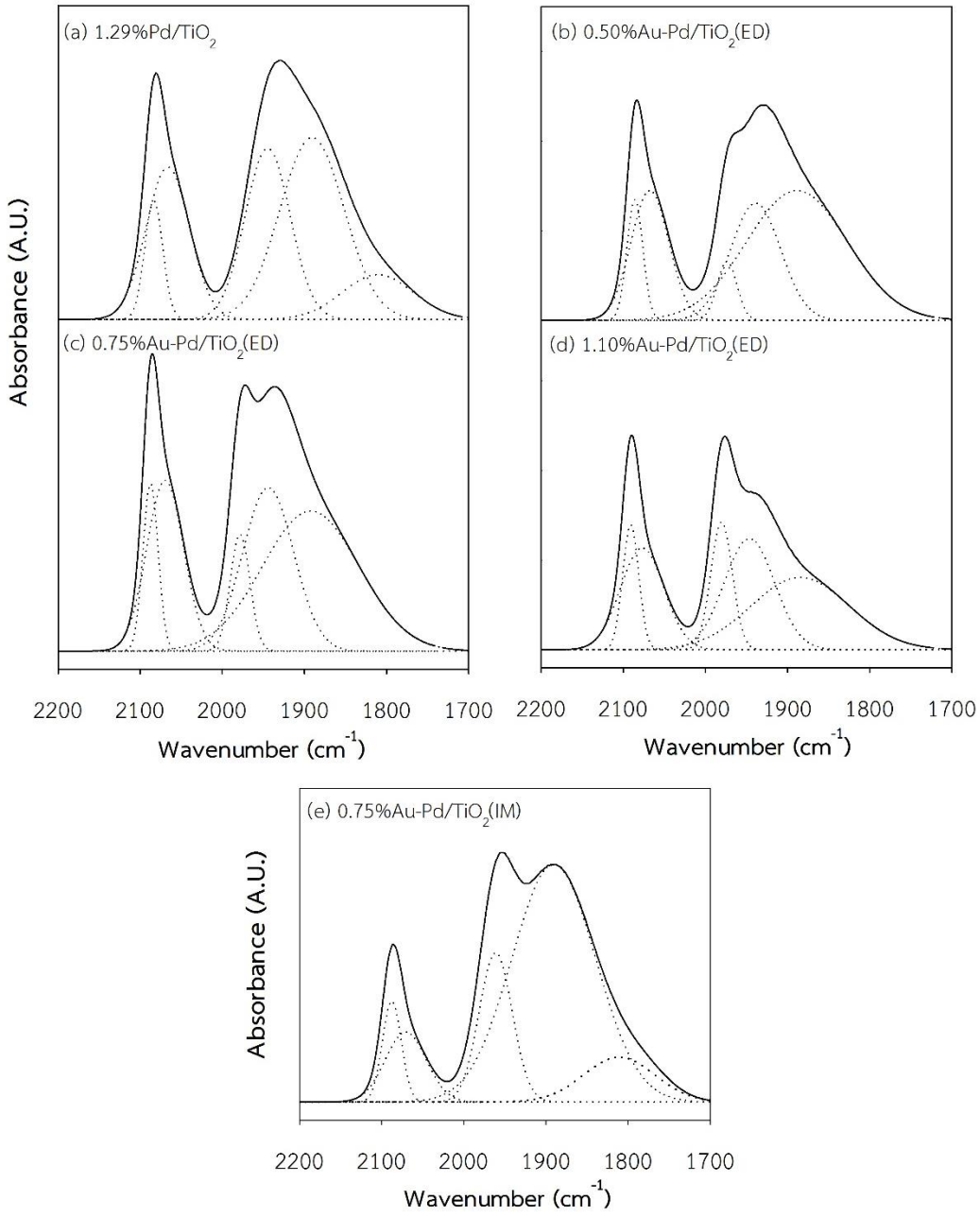

Figure 4.9 FTIR spectra of adsorbed CO at room temperature of Pd/TiO_2 and Au-Pd/TiO_2 bimetallic catalysts.

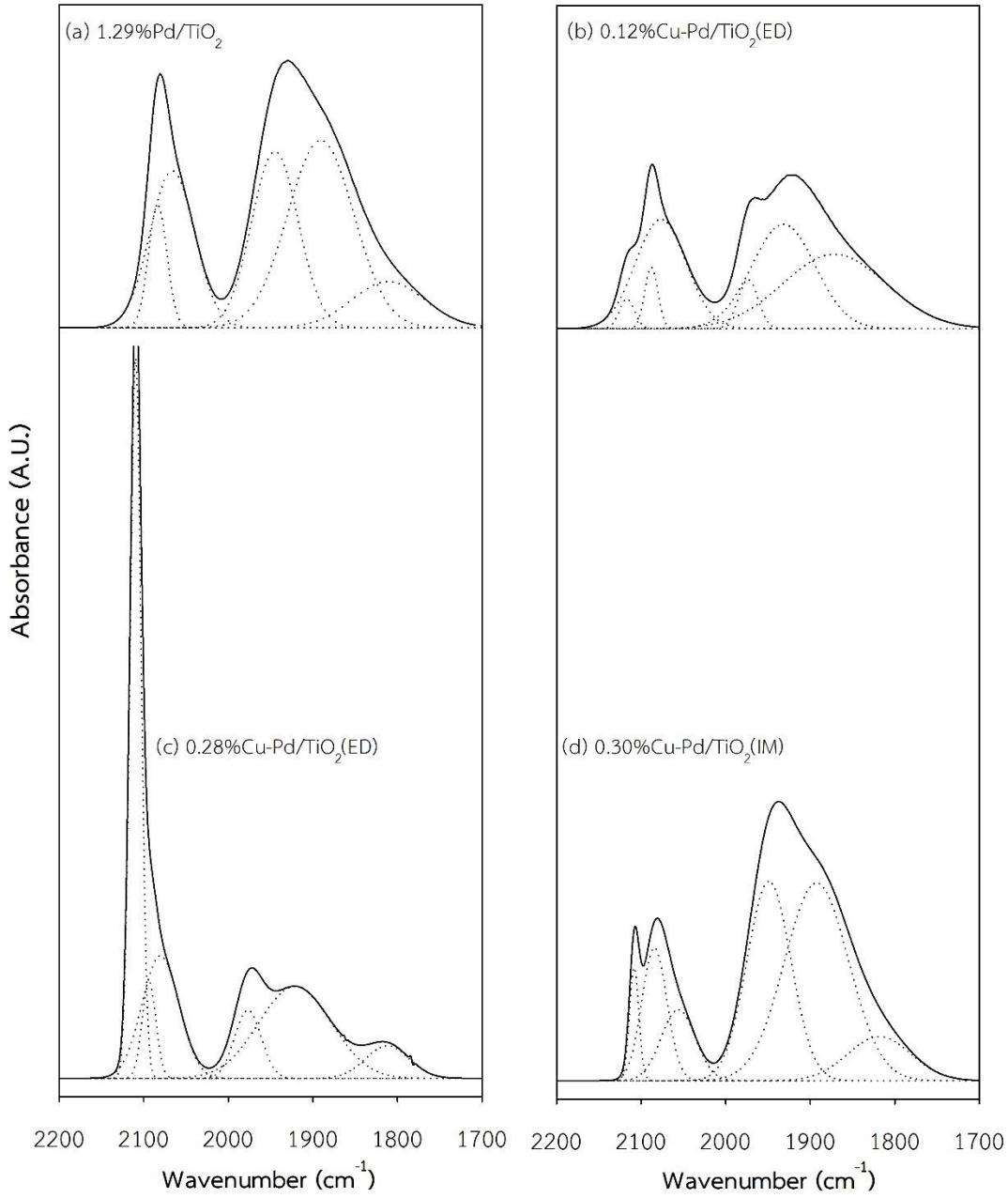

Figure 4.10 FTIR spectra of adsorbed CO at 30 °C of Pd/TiO_2 and $Cu\text{-}Pd/TiO_2$ bimetallic catalysts.

Table 4.2 FTIR peak position and intensity ratios of Pd/TiO_2, $Au-Pd/TiO_2$ and $Cu-Pd/TiO_2$ bimetallic

Samples	ML on Pd	Cu/Cu^+	Linear region(L)		Bridge region(NL)			Linear/ Bridge	L1/L2
			L1	L2	NL1	NL2	NL3		
Pd/TiO_2	-	-	2083	2066	1945	1891	1811	0.387	0.321
0.50%$Au-Pd/TiO_2$(ED)	0.15	-	2086	2068	1974	1939	1888	0.340	0.391
0.75%Au-Pd/TiO2(ED)	0.55	-	2087	2070	1978	1944	1892	0.366	0.403
1.10%$Au-Pd/TiO_2$(ED)	0.59	-	2091	2077	1980	1946	1885	0.417	0.452
0.75%$Au-Pd/TiO_2$(IM)	0.15	-	2088	2071	1961	1891	1784	0.180	0.663
0.12%$Cu-Pd/TiO_2$(ED)	0.37	2117	2088	2077	1974	1932	1871	0.416	0.145
0.30%$Cu-Pd/TiO_2$(ED)	0.54	2110	2097	2070	1972	1914	1811	0.594	0.294
0.30%$Cu-Pd/TiO_2$(IM)	0.24	2108	2084	2056	1949	1892	1818	0.237	1.374

The FTIR spectra of Pd/TiO_2, $Au-Pd/TiO_2$ and $Cu-Pd/TiO_2$ are shown in Figure 4.9 and **Figure 4.10**. For all cases the intensities of bridging CO-Pd bands decreased due to dilution of Pd surface by deposition of Au or Cu. Nevertheless, In case of catalysts prepared by incipient wetness impregnation method, intensities of bridging CO-Pd bands decreased slightly compared to electroless deposition method. It is obvious that Au or Cu likely deposited on titania support or accumulated on the second metal particles.

The relative intensities of linear to bridged peaks (L/NL) were increased by addition second metal. This is an indication that Au or Cu selective deposition on three-fold, bridging Pd sites. In addition, **Table 4.2** shows that the relative intensity ratios (L1/L2) linear CO peak of CO-Pd(111) to CO-Pd(100), decreased with Cu wt.% loading. It may be expected that preferential deposition on Pd(111) surfaces, while Au is not selective. A possible explanation was that electroless deposition of Cu using an ED bath composed of Cu^{2+} ions and HCHO as the reducing agent resulted in preferential deposition on Pd(111) surfaces [58].

4.2.5 XPS

The binding energy of Au in bimetallic catalyst were measured by XPS and are shown in **Figure 4.11**. For the Au-Pd/TiO_2 prepared by ED method, the B.E. of Au metal is lower than the typical metallic gold (B.E. 84.0 ± 0.1 eV). In **Table 4.3**, as the surface coverage of Au metal on Pd increased, the B.E. shifts of Au $4f_{7/2}$ decrease with coverage because the higher surface coverage of Au loading resulted in autocatalytic deposition to form aggregates of Au on Pd, similar to the metal particles of the supported monometallic gold catalyst [51]. Thus, the B.E. shift was maximized at the lowest coverage of Au since the Au metal were essentially distribution in a monodisperse manner on the Pd surface to give the maximum e^- transfer from Pd to the Au metal. Likewise, impregnation method had accumulation of Au particle to obtain B.E. similar to metallic gold. The B.E. of Au-Pd/TiO_2 prepared by IM method higher Au metallic gold (+1.5 eV) because of Au in state of Au^{1+}.

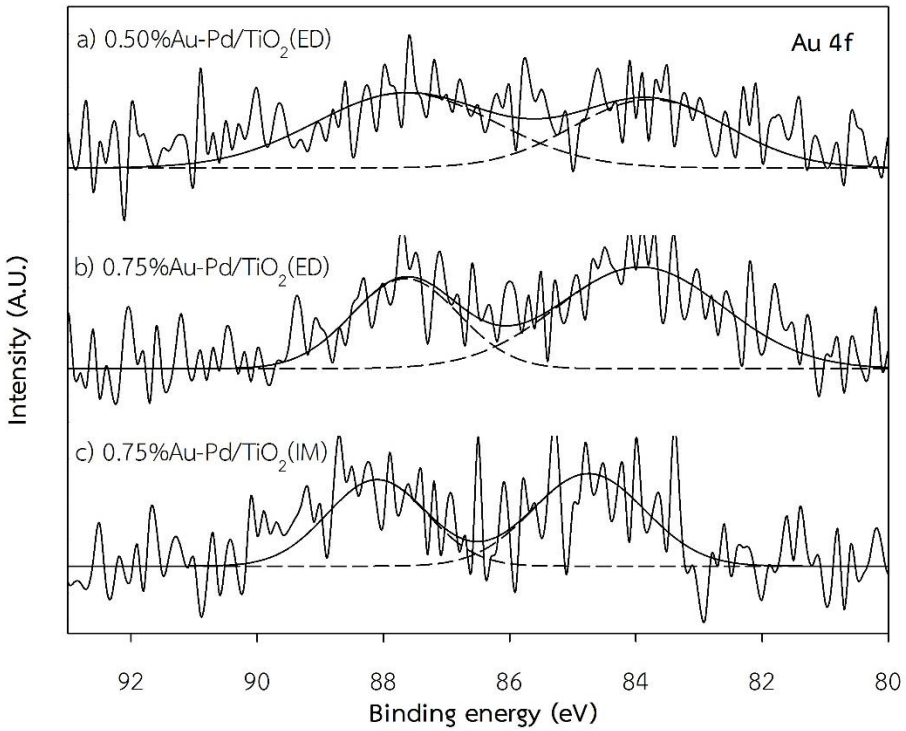

Figure 4.11 XPS Au 4f core level spectra of Au-Pd/TiO_2.

The B.E. of Pd are shown in **Table 4.3.** The Pd 3d5/2 spectra were detected at 335.4-336.7 eV which could be attributed to the presence of PdO and Pd^0. The B.E. of Pd for bimetallic catalyst shift from Pd/TiO_2 monometallic catalyst indicates the surface enrichment of second metal on Pd/TiO_2.

Table 4.3 Peak position from XPS spectra.

Catalysts	coverage	B.E.(eV) of Pd		B.E.(eV) of Au	
		$3d_{3/2}$	$3d_{5/2}$	$4f_{5/2}$	$4f_{7/2}$
1.286%Pd/TiO_2	-	340.8	335.4	-	-
0.50%Au-Pd/TiO_2(ED)	0.31	340.2	335.4	87.7	82.9
0.75%Au-Pd/TiO_2(ED)	0.55	340.8	335.0	86.9	83.1
0.75%Au-Pd/TiO_2(IM)	0.15	341.3	336.5	87.3	85.5
0.10%Cu-Pd/TiO_2(ED)	0.30	340.1	335.9	-	-
0.28%Cu-Pd/TiO_2(ED)	0.54	342.3	336.7	-	-
0.30%Cu-Pd/TiO_2(IM)	0.24	342.1	335.4	-	-

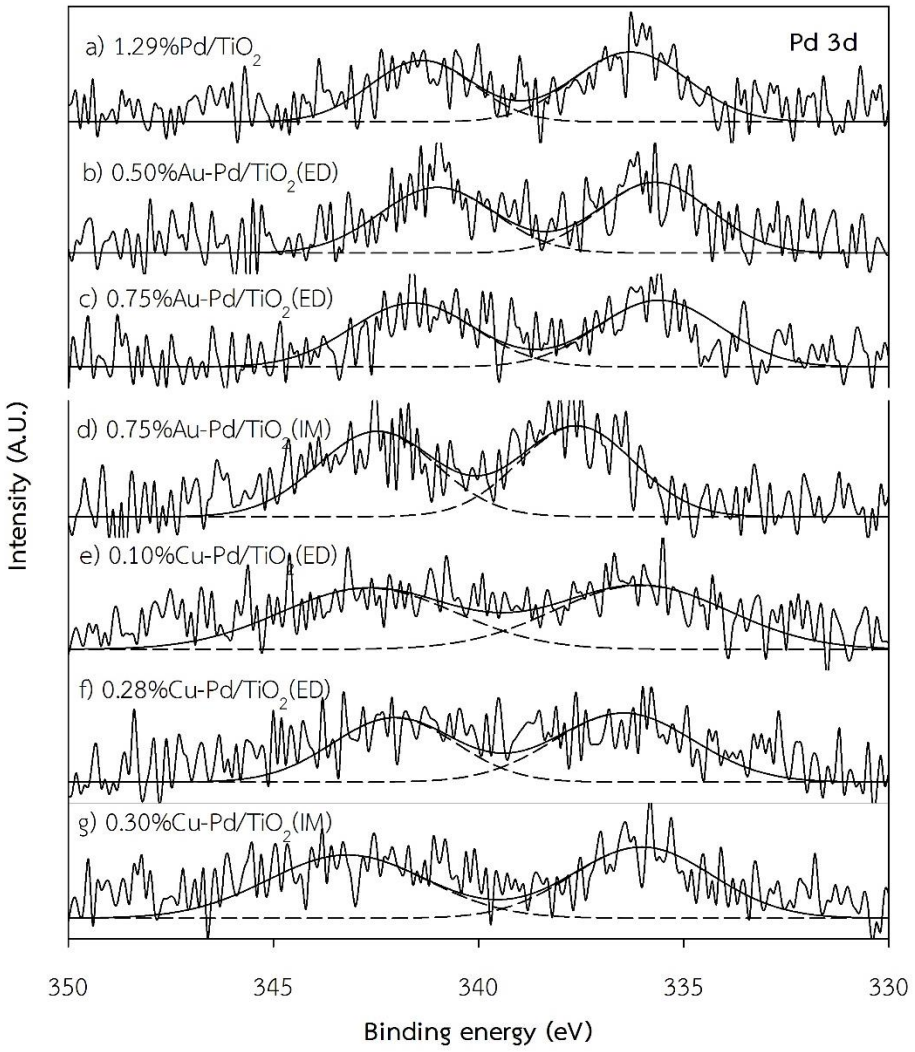

Figure 4.12 XPS Pd 3d core level spectra of Pd/TiO_2, $Au-Pd/TiO_2$ and $Cu-Pd/TiO_2$.

4.2.6 TEM

The TEM images of TiO_2 support, Pd/TiO_2, $Au-Pd/TiO_2$ and $Cu-Pd/TiO_2$ are shown in **Figure 4.13** and **Figure 4.14**. The TiO_2 particle showed spherical shape and no change crystallite size after both palladium and second metal loading. The average crystallite size determined by TEM analyses was around 17-19 nm, which were consistent with the XRD result. It is difficult to found Pd or PdO clusters on TiO_2 support when Pd was added by strong electrostatic adsorption method. This can be due to vary small particle size or well distribution of Pd on TiO_2. However, after addition of a second metal on Pd, some agglomeration of second metal on Pd surface can be seen.

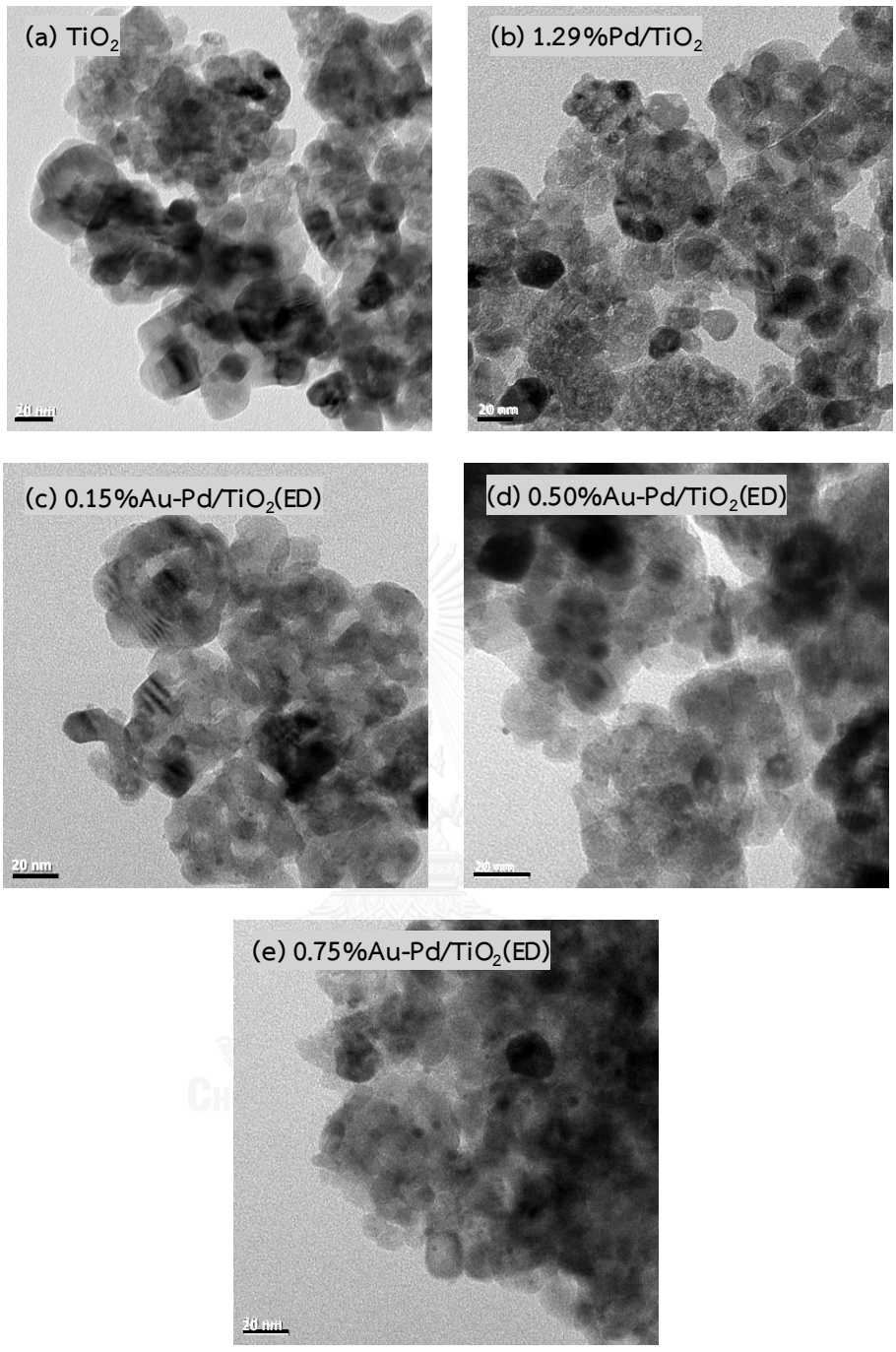

Figure 4.13 TEM images of TiO_2, Pd/TiO_2 and $Au\text{-}Pd/TiO_2$ catalysts.

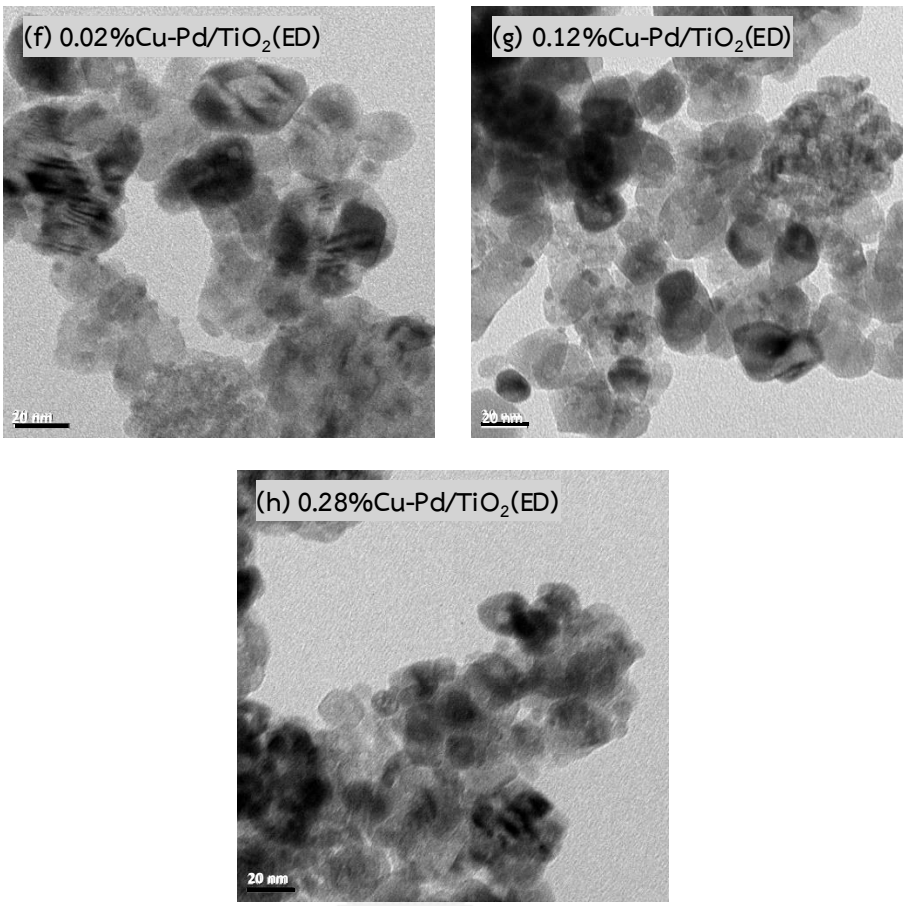

Figure 4.14 TEM images of Cu-Pd/TiO_2 catalysts.

4.3 Reaction study in selective hydrogenation of acetylene

The catalytic performance of monometallic and bimetallic catalysts were investigated in the selective hydrogenation of acetylene at various reaction temperatures from 40 °C to 100 °C. Acetylene conversion is defined as a mole of acetylene converted with respect to acetylene in feed. Ethylene selectivity is defined as the percentage of acetylene hydrogenation to ethylene over totally hydrogenated acetylene. The ethylene being hydrogenated to ethane (ethylene loss) is the different between all the hydrogen consumed and all acetylene which has been totally hydrogenated [59]. The conversion plots are shown in **Figure 4.15** and **Figure 4.16**, acetylene conversion increased with increasing temperature while ethylene selectivity slightly increased for both monometallic and bimetallic catalysts. The conversion of Pd/TiO_2 was 82% at 40 °C and reached 93% at 100 °C, while selectivity was ranging from 62% to 68%. Addition of Au or Cu on Pd surface can improved conversion to 100% at Au coverage of 0.55 and Cu coverage of 0.54. It is suggested that adsorption of acetylene on Au and Cu resulted to increasing activity of bimetallic catalysts [60]. Similarly, bimetallic catalysts can improve ethylene selectivity to 79% for both Au-Pd/TiO_2 and Cu-Pd/TiO_2. Because the coverage of Au or Cu on the Pd surface can systematically changed by electroless deposition, it is possible to observe the transition from multi-σ to π- adsorbed species. At low coverages of Au and Cu on Pd, there was an abundance of contiguous Pd surface sites where the strongly adsorbed acetylene and ethylene were adsorbed as multi-σ - adsorbed specie. These species favor hydrogenation of acetylene to form ethane more than ethylene. In this study, acetylene was more weakly adsorbed as a adsorbed π- species requiring potentially only single Pd surface site, which favored formation of ethylene [3]. This is in accordance with FTIR of adsorbed CO on Pd surfaces result that the intensity ratio of linear to bridged (L/NL) decreased with higher Au or Cu coverage on Pd surface.

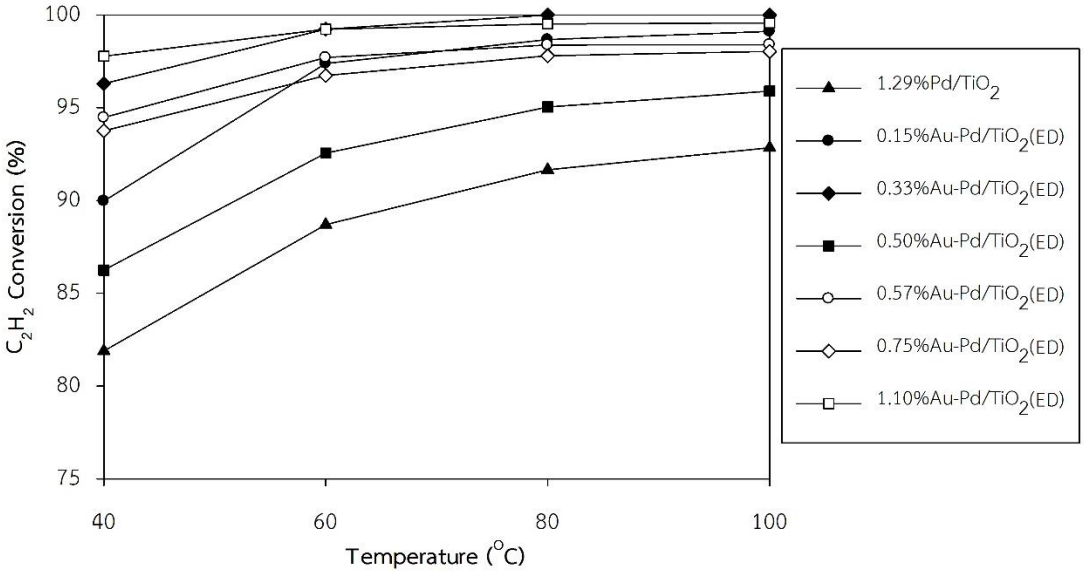

Figure 4.15 Acetylene conversion as a function of reaction temperature for Pd/TiO_2 and Au-Pd/TiO_2 catalyst prepared by electroless deposition method.

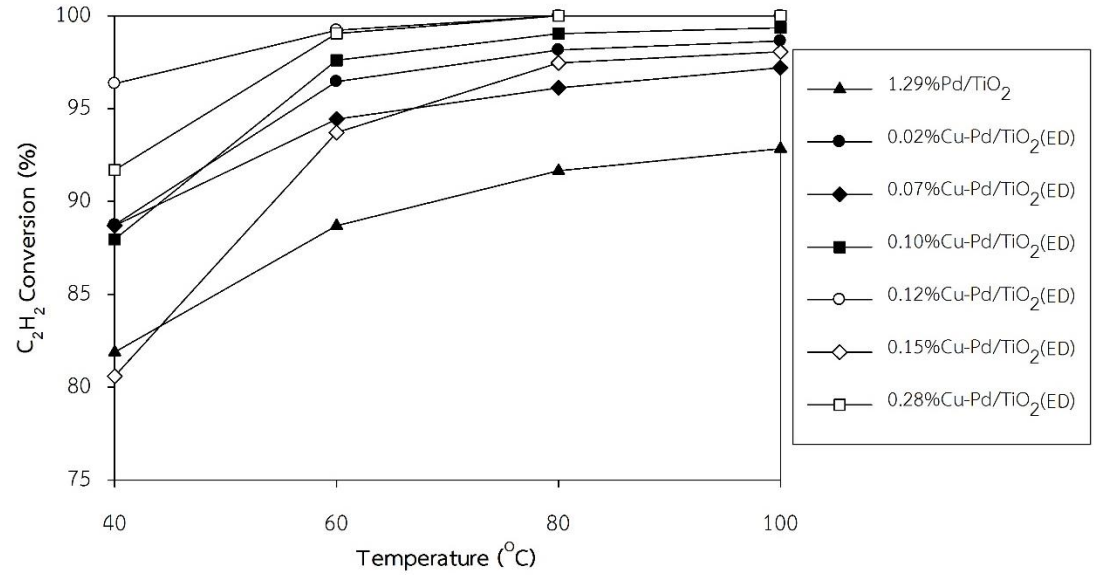

Figure 4.16 Acetylene conversion as a function of reaction temperature for Pd/TiO_2 and Cu-Pd/TiO_2 catalyst prepared by electroless deposition method.

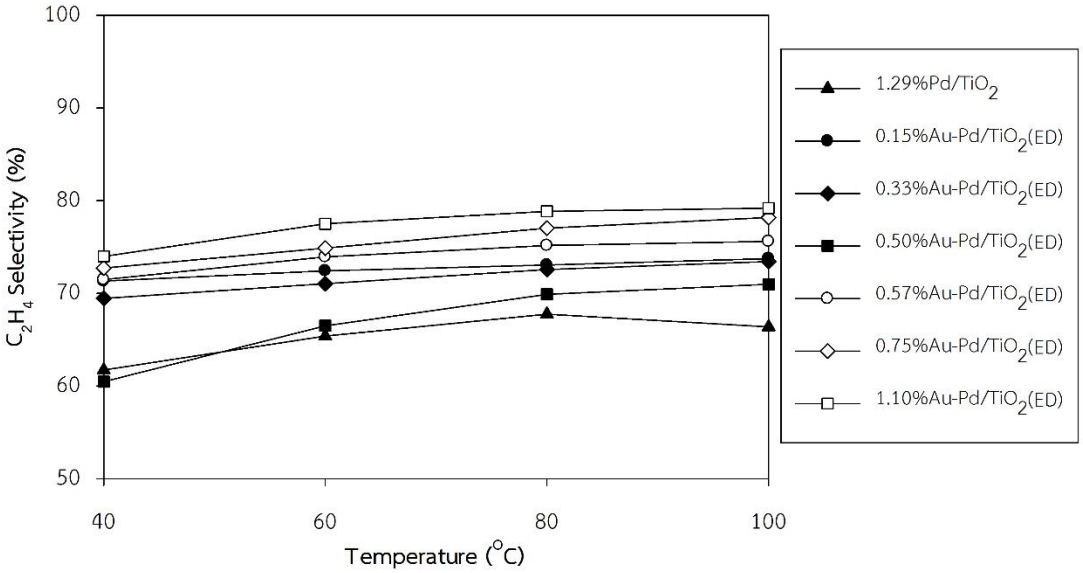

Figure 4.17 Ethylene selectivity as a function of reaction temperature for Pd/TiO_2 and $Au\text{-}Pd/TiO_2$ catalyst prepared by electroless deposition method.

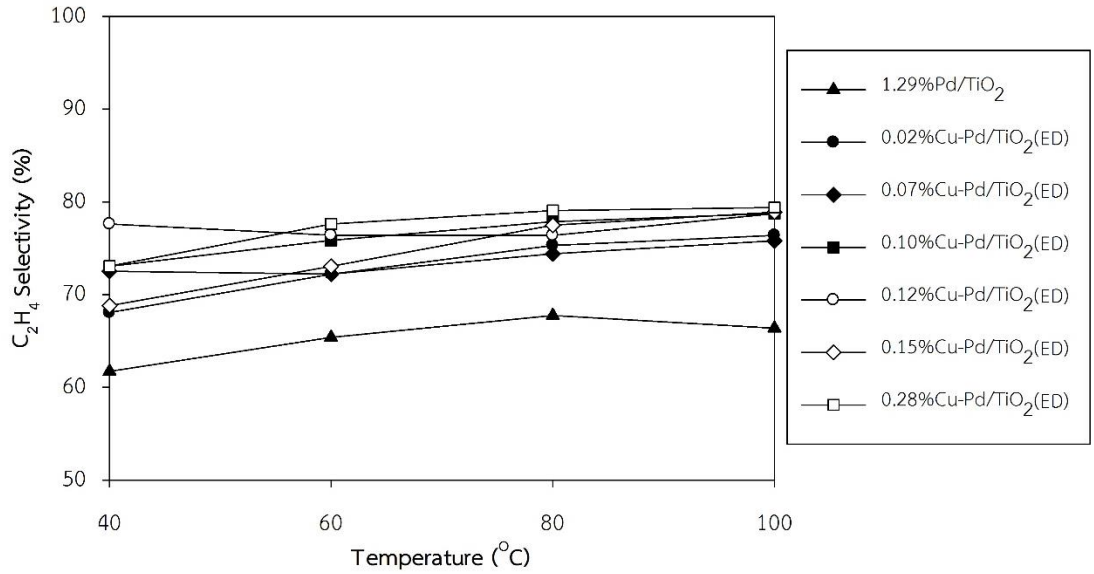

Figure 4.18 Ethylene selectivity as a function of reaction temperature for Pd/TiO_2 and $Cu\text{-}Pd/TiO_2$ catalyst prepared by electroless deposition method.

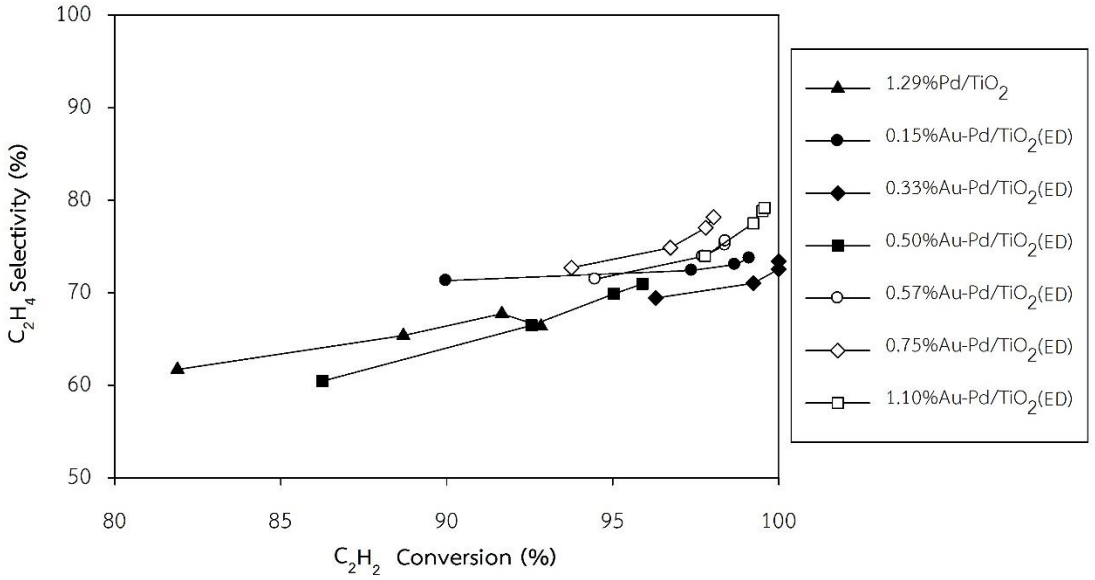

Figure 4.19 The catalytic performance of Pd/TiO_2 and $Au\text{-}Pd/TiO_2$ catalyst prepared by electroless deposition method in selective hydrogenation of acetylene.

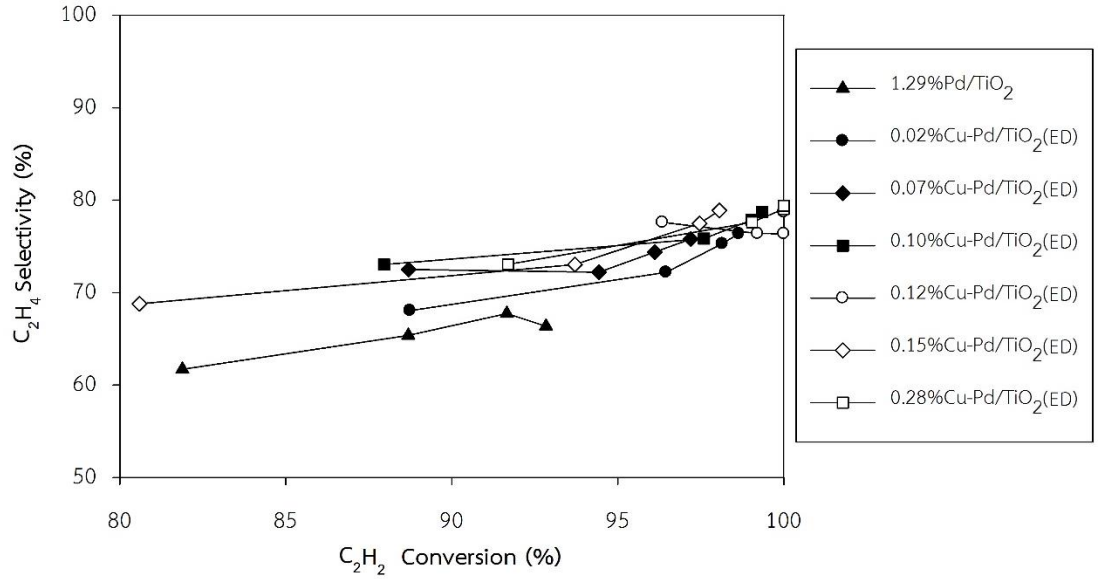

Figure 4.20 The catalytic performance of Pd/TiO_2 and $Cu\text{-}Pd/TiO_2$ catalyst prepared by electroless deposition method in selective hydrogenation of acetylene.

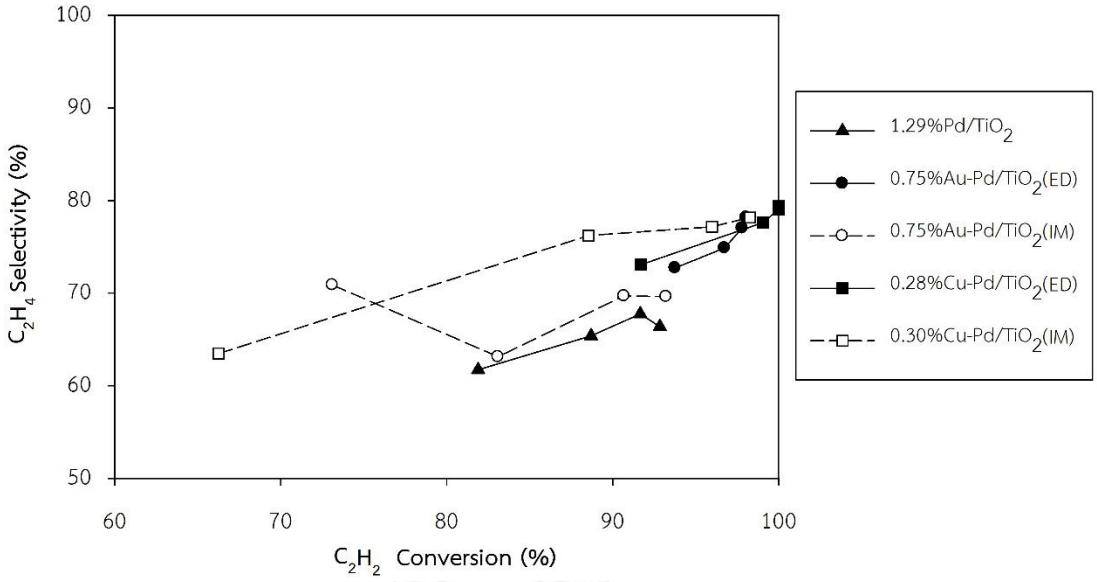

Figure 4.21 The catalytic performance of Pd/TiO2, Au-Pd/TiO_2 and Cu-Pd/TiO_2 catalyst prepared by electroless deposition method and incipient wetness impregnation method in selective hydrogenation of acetylene.

The catalytic performances of Pd/TiO_2, Au-Pd/TiO_2 and Cu-Pd/TiO_2 catalysts prepared by electroless deposition method compared with incipient wetness impregnation method are shown in **Figure 4.21**. Coverage of Au or Cu on Pd surface prepared by electroless deposition method can improve both acetylene conversion and ethylene selectivity more than those prepared by incipient wetness impregnation method, this is probably due to the electroless deposition method could decrease abundance of contiguous Pd surface sites which is strongly affected by acetylene adsorbed as **TT-** adsorbed species more than impregnation method. It was observed that ethylene selectivity of bimetallic catalysts prepared by electroless deposition method was higher than those prepared by incipient wetness impregnation method.

CHAPTER 5
CONCLUSIONS AND RECOMMENDATIONS

5.1 Conclusion

1. The 1.29 wt.%Pd/TiO_2 catalyst prepared by strong electrostatic adsorption showed high Pd dispersion at 37.9%. The strong electrostatic adsorption method appears to be a rational procedure for the cheap, simple, and scalable preparation of highly dispersed Pd on titania support.

2. The preparation of bimetallic catalysts by electroless deposition method has shown to be a good method with controlled coverage of Au or Cu on Pd surface. Selectivity of acetylene to ethylene were enhanced at high coverage of second metal on Pd surface, due to change of the transition of adsorption mode of acetylene on Pd surface from strongly multi-**σ** -adsorbed on large Pd ensembles to weakly adsorbed, **π**- adsorbed species on small Pd ensembles.

3. The Cu-Pd/TiO_2 catalysts prepared by ED showed higher ethylene selectivity and hydrogenation activity than the Au-Pd/TiO_2 catalysts. The results from CO-IR suggested that Cu selective deposited preferentially onto the low-coordination sites than Au which inhibited fully hydrogenation of ethylene to ethane.

5.2 Recommendations

1. Other bimetallic modified on Pd/TiO_2 catalysts prepared by electroless deposition method should be studied in the future work.

2. The temperature program desorption of ethylene should be studied for comparison of the ability to absorb and desorb ethylene of catalysts.

REFERENCES

[1] Benavidez, A.D., et al. Improved selectivity of carbon-supported palladium catalysts for the hydrogenation of acetylene in excess ethylene. Applied Catalysis A: General 482 (2014): 108-115.

[2] Azizi, M., Zolfaghari Sharak, A., Mousavi, S.A., Bakhtiari Ziabari, F., Shariati, J., and Azizi, S. STUDY ON THE ACETYLENE HYDROGENATION PROCESS FOR ETHYLENE PRODUCTION: SIMULATION, MODIFICATION, AND OPTIMIZATION. Chemical Engineering Communications 200(7) (2013): 863-877.

[3] Zhang, Y., Diao, W., Williams, C.T., and Monnier, J.R. Selective hydrogenation of acetylene in excess ethylene using Ag- and Au–Pd/SiO_2 bimetallic catalysts prepared by electroless deposition. Applied Catalysis A: General 469 (2014): 419-426.

[4] Kim, S.K., Lee, J.H., Ahn, I.Y., Kim, W.-J., and Moon, S.H. Performance of Cu-promoted Pd catalysts prepared by adding Cu using a surface redox method in acetylene hydrogenation. Applied Catalysis A: General 401(1–2) (2011): 12-19.

[5] Kim, W.-J. and Moon, S.H. Modified Pd catalysts for the selective hydrogenation of acetylene. Catalysis Today 185(1) (2012): 2-16.

[6] Leviness, S., Nair, V., Weiss, A.H., Schay, Z., and Guczi, L. Acetylene hydrogenation selectivity control on PdCu/Al_2O_3 catalysts. Journal of Molecular Catalysis 25(1–3) (1984): 131-140.

[7] Kang, J.H., Shin, E.W., Kim, W.J., Park, J.D., and Moon, S.H. Selective hydrogenation of acetylene on Pd/SiO_2 catalysts promoted with Ti, Nb and Ce oxides. Catalysis Today 63(2–4) (2000): 183-188.

[8] Kang, J.H., Shin, E.W., Kim, W.J., Park, J.D., and Moon, S.H. Selective Hydrogenation of Acetylene on TiO2-Added Pd Catalysts. Journal of Catalysis 208(2) (2002): 310-320.

[9] Jiao, L. and Regalbuto, J.R. The synthesis of highly dispersed noble and base metals on silica via strong electrostatic adsorption: I. Amorphous silica. Journal of Catalysis 260(2) (2008): 329-341.

[10] Rebelli, J., Detwiler, M., Ma, S., Williams, C.T., and Monnier, J.R. Synthesis and characterization of Au–Pd/SiO_2 bimetallic catalysts prepared by electroless deposition. Journal of Catalysis 270(2) (2010): 224-233.

[11] Kraeutler, B. and Bard, A.J. Heterogeneous photocatalytic preparation of supported catalysts. Photodeposition of platinum on titanium dioxide powder and other substrates. Journal of the American Chemical Society 100(13) (1978): 4317-4318.

[12] Eschemann, T.O., Bitter, J.H., and de Jong, K.P. Effects of loading and synthesis method of titania-supported cobalt catalysts for Fischer–Tropsch synthesis. Catalysis Today 228 (2014): 89-95.

[13] Mor, G.K., Shankar, K., Paulose, M., Varghese, O.K., and Grimes, C.A. Use of Highly-Ordered TiO2 Nanotube Arrays in Dye-Sensitized Solar Cells. Nano Letters 6(2) (2006): 215-218.

[14] D'Agata, A., et al. Enhanced toxicity of 'bulk' titanium dioxide compared to 'fresh' and 'aged' nano-TiO_2 in marine mussels (Mytilus galloprovincialis). Nanotoxicology 8(5) (2014): 549-558.

[15] Guo, Y.G., Hu, Y.S., Sigle, W., and Maier, J. Superior Electrode Performance of Nanostructured Mesoporous TiO_2 (Anatase) through Efficient Hierarchical Mixed Conducting Networks. Advanced Materials 19(16) (2007): 2087-2091.

[16] Xu, J., Li, K., Shi, W., Li, R., and Peng, T. Rice-like brookite titania as an efficient scattering layer for nanosized anatase titania film-based dye-sensitized solar cells. Journal of Power Sources 260 (2014): 233-242.

[17] Chen, M.-m., Sun, X., Qiao, Z.-j., Ma, Q.-q., and Wang, C.-y. Anatase-TiO_2 nanocoating of $Li_4Ti_5O_{12}$ nanorod anode for lithium-ion batteries. Journal of Alloys and Compounds 601 (2014): 38-42.

[18] Fujimoto, M., et al. TiO_2 anatase nanolayer on TiN thin film exhibiting high-speed bipolar resistive switching. Applied Physics Letters 89(22) (2006): 223509.

[19] Grosso, D., et al. Highly Porous TiO_2 Anatase Optical Thin Films with Cubic Mesostructure Stabilized at 700 °C. Chemistry of Materials 15(24) (2003): 4562-4570.

[20] Ramimoghadam, D., Bagheri, S., and Abd Hamid, S.B. Biotemplated synthesis of anatase titanium dioxide nanoparticles via lignocellulosic waste material. Biomed Res Int 2014 (2014): 205636.

[21] Wang, J., Polleux, J., Lim, J., and Dunn, B. Pseudocapacitive Contributions to Electrochemical Energy Storage in TiO_2 (Anatase) Nanoparticles. The Journal of Physical Chemistry C 111(40) (2007): 14925-14931.

[22] Kominami, H., et al. Novel synthesis of microcrystalline titanium(IV) oxide having high thermal stability and ultra-high photocatalytic activity: thermal decomposition of titanium(IV) alkoxide in organic solvents. Catalysis Letters 46(3-4) (1997): 235-240.

[23] Bamwenda, G.R., Tsubota, S., Nakamura, T., and Haruta, M. The influence of the preparation methods on the catalytic activity of platinum and gold supported on TiO_2 for CO oxidation. Catalysis Letters 44(1-2) (1997): 83-87.

[24] Tauster, S.J., Fung, S.C., Baker, R.T.K., and Horsley, J.A. Strong Interactions in Supported-Metal Catalysts. Science 211(4487) (1981): 1121-1125.

[25] Kim, T.S., Stiehl, J.D., Reeves, C.T., Meyer, R.J., and Mullins, C.B. Cryogenic CO Oxidation on TiO_2-Supported Gold Nanoclusters Precovered with Atomic Oxygen. Journal of the American Chemical Society 125(8) (2003): 2018-2019.

[26] Lietti, L., Forzatti, P., and Bregani, F. Steady-State and Transient Reactivity Study of TiO_2-Supported V_2O_5–WO_3 De-NOx Catalysts: Relevance of the Vanadium–Tungsten Interaction on the Catalytic Activity. Industrial & Engineering Chemistry Research 35(11) (1996): 3884-3892.

[27] Lin, S.D., Bollinger, M., and Vannice, M.A. Low temperature CO oxidation over Au/TiO_2 and Au/SiO_2 catalysts. Catalysis Letters 17(3): 245-262.

[28] Amores, J.M.G., Escribano, V.S., and Busca, G. Anatase crystal growth and phase transformation to rutile in high-area TiO_2, MoO_3-TiO_2 and other TiO_2-supported oxide catalytic systems. Journal of Materials Chemistry 5(8) (1995): 1245-1249.

[29] Yan, W., Mahurin, S.M., Pan, Z., Overbury, S.H., and Dai, S. Ultrastable Au Nanocatalyst Supported on Surface-Modified TiO_2 Nanocrystals. Journal of the American Chemical Society 127(30) (2005): 10480-10481.

[30] Ren, X., Zhang, H., and Cui, Z. Acetylene decomposition to helical carbon nanofibers over supported copper catalysts. Materials Research Bulletin 42(12) (2007): 2202-2210.

[31] Park, K.-W. and Seol, K.-S. Nb-TiO_2 supported Pt cathode catalyst for polymer electrolyte membrane fuel cells. Electrochemistry Communications 9(9) (2007): 2256-2260.

[32] Palcheva, R., Dimitrov, L., Tyuliev, G., Spojakina, A., and Jiratova, K. TiO_2 nanotubes supported NiW hydrodesulphurization catalysts: Characterization and activity. Applied Surface Science 265 (2013): 309-316.

[33] Nolan, M. Modifying ceria (111) with a TiO_2 nanocluster for enhanced reactivity. The Journal of Chemical Physics 139(18) (2013): 184710.

[34] Yan, W., et al. Preparation and Comparison of Supported Gold Nanocatalysts on Anatase, Brookite, Rutile, and P25 Polymorphs of TiO_2 for Catalytic Oxidation of CO. The Journal of Physical Chemistry B 109(21) (2005): 10676-10685.

[35] Went, G.T., Leu, L.-j., and Bell, A.T. Quantitative structural analysis of dispersed vanadia species in TiO2(anatase)-supported V_2O_5. Journal of Catalysis 134(2) (1992): 479-491.

[36] Francisco, M.S.P. and Mastelaro, V.R. Inhibition of the Anatase−Rutile Phase Transformation with Addition of CeO_2 to CuO−TiO_2 System: Raman Spectroscopy, X-ray Diffraction, and Textural Studies. Chemistry of Materials 14(6) (2002): 2514-2518.

[37] Bagheri, S., Shameli, K., and Abd Hamid, S.B. Synthesis and Characterization of Anatase Titanium Dioxide Nanoparticles Using Egg White Solution via Sol-Gel Method. Journal of Chemistry 2013 (2013): 1-5.

[38] McCue, A.J. and Anderson, J.A. Recent advances in selective acetylene hydrogenation using palladium containing catalysts. Frontiers of Chemical Science and Engineering 9(2) (2015): 142-153.

[39] García-Mota, M., et al. A density functional theory study of the 'mythic' Lindlar hydrogenation catalyst. Theoretical Chemistry Accounts 128(4-6) (2010): 663-673.

[40] Bridier, B., Lopez, N., and Perez-Ramirez, J. Molecular understanding of alkyne hydrogenation for the design of selective catalysts. Dalton Transactions 39(36) (2010): 8412-8419.

[41] Segura, Y., Lopez, N., and Perezramirez, J. Origin of the superior hydrogenation selectivity of gold nanoparticles in alkyne + alkene mixtures: Triple- versus double-bond activation. Journal of Catalysis 247(2) (2007): 383-386.

[42] Shin, E.W., Choi, C.H., Chang, K.S., Na, Y.H., and Moon, S.H. Properties of Si-modified Pd catalyst for selective hydrogenation of acetylene. Catalysis Today 44(1–4) (1998): 137-143.

[43] Kim, W. Deactivation behavior of a TiO_2-added Pd catalyst in acetylene hydrogenation. Journal of Catalysis 226(1) (2004): 226-229.

[44] Kontapakdee, K., Panpranot, J., and Praserthdam, P. Effect of Ag addition on the properties of Pd–Ag/TiO_2 catalysts containing different TiO2 crystalline phases. Catalysis Communications 8(12) (2007): 2166-2170.

[45] John, R.R. Strong Electrostatic Adsorption of Metals onto Catalyst Supports. in Catalyst Preparation, pp. 297-318: CRC Press, 2006.

[46] John, R.R. A Scientific Method to Prepare Supported Metal Catalysts. in Surface and Nanomolecular Catalysis, pp. 161-194: CRC Press, 2006.

[47] Jiao, L. and Regalbuto, J.R. The synthesis of highly dispersed noble and base metals on silica via strong electrostatic adsorption: II. Mesoporous silica SBA-15. Journal of Catalysis 260(2) (2008): 342-350.

[48] D'Souza, L. and Regalbuto, J.R. Strong electrostatic adsorption for the preparation of Pt/Co/C and Pd/Co/C bimetallic electrocatalysts. 175 (2010): 715-718.

[49] Stojan S. Djoki´c and Cavallotti, P.L. ELECTROLESS DEPOSITION: THEORY AND APPLICATIONS. in MODERN ASPECTS OF ELECTROCHEMISTRY, No. 48 ELECTRODEPOSITION, pp. 251-285.

[50] Perminder Bindra and White, J.R. Fundamental Aspects of Electroless Copper Plating. in Electroless Plating - Fundamentals and Applications, pp. 289-329, 1990.

[51] Rebelli, J., Rodriguez, A.A., Ma, S., Williams, C.T., and Monnier, J.R. Preparation and characterization of silica-supported, group IB–Pd bimetallic catalysts prepared by electroless deposition methods. Catalysis Today 160(1) (2011): 170-178.

[52] Rodriguez, A.A., Williams, C.T., and Monnier, J.R. Selective liquid-phase oxidation of glycerol over Au–Pd/C bimetallic catalysts prepared by electroless deposition. Applied Catalysis A: General 475 (2014): 161-168.

[53] Benson, J.E., Hwang, H.S., and Boudart, M. Hydrogen-oxygen titration method for the measurement of supported palladium surface areas. Journal of Catalysis 30(1) (1973): 146-153.

[54] Giorgi, J.B., Schroeder, T., Bäumer, M., and Freund, H.-J. Study of CO adsorption on crystalline-silica-supported palladium particles. Surface Science 498(1–2) (2002): L71-L77.

[55] Szanyi, J., Kuhn, W.K., and Goodman, D.W. CO Adsorption on Pd(111) and Pd(100): Low and High Pressure Correlations. Journal of Vacuum Science and Technology A: Vacuum, Surfaces and Films 11(4) (1993): 1969-1974.

[56] Wadayama, T., Abe, K., and Osano, H. Infrared reflection absorption study of carbon monoxide adsorption on Pd/Cu(1 1 1). Applied Surface Science 253(5) (2006): 2540-2546.

[57] Bradshaw, A.M. and Hoffmann, F.M. The chemisorption of carbon monoxide on palladium single crystal surfaces: IR spectroscopic evidence for localised site adsorption. Surface Science 72(3) (1978): 513-535.

[58] Schaal, M.T., et al. Hydrogenation of 3,4-epoxy-1-butene over Cu-Pd/SiO_2 catalysts prepared by electroless deposition. Catalysis Today 123(1-4) (2007): 142-150.

[59] Riyapan, S., et al. Improved catalytic performance of Pd/TiO_2 in the selective hydrogenation of acetylene by using H_2-treated sol–gel TiO_2. Journal of Molecular Catalysis A: Chemical 383–384 (2014): 182-187.

[60] Trimm, D.L. Design of industrial catalysts. Elsevier Scientific Pub. Co., 1980.

APPENDIX

APPENDIX A
CACULATION FOR CATALYST PREPARATION

The calculation shown below for Pd/TiO_2 prepared by strong electrostatic adsorption method and $Au\text{-}Pd/TiO_2$ and $Cu\text{-}Pd/TiO_2$ catalysts prepared by electroless deposition and incipient wetness impregnation method.

1. Calculation of Pd support on titania supports by strong electrostatic adsorption method.

Uptake-pH surveys used Pd metal solution of 200 ppm and surface loading were 1000 m^2/L for TiO_2. Base on 1000 mL of Pd solution used; the composition of the catalyst will be as follows:

Reagent: - Titanium dioxide (TiO_2)

Surface area = 50 m^2/g

- Tetraamminepalladium(II) chloride monohydrate ($Pd(NH_3)_4Cl_2.H_2O$)

Molecular weight = 263.46 g/mol

Weight of $Pd(NH_3)_4Cl_2.H_2O$ required

$$= \frac{\text{Pd metal solution} \times \text{solution required} \times \text{M.W. of } Pd(NH_3)_4Cl_2.H_2O}{\text{M.W. of Pd}}$$

$$= \frac{200\ mg/L \times 1000\ mL \times 263.46\ g/mol}{106.42\ g/mol} = 0.495\ g$$

For uptake-pH surveys were conducted in flask containing 20 mL of 200 ppm Pd solution, thus TiO_2 required as follow:

$$TiO_2 \text{ required} = \frac{\text{solution required} \times \text{surface loading}}{\text{surface area of } TiO_2}$$

$$= \frac{20\ mL \times 1000\ m^2/L}{50\ m^2/g} = 0.4\ g \text{ of } TiO_2$$

2. Calculation of Au and Cu on Pd/TiO_2 by electroless deposition method.

For Au on Pd/TiO_2 used Potassium dicyanoaurate(I) as the metal sources and hydrazine as the reducing agent. The volume of the electroless bath was 100 mL for 1 g of Pd/TiO_2.

Initial concentration of metal salts were selected based on the desired the theoretical coverage of Au on Pd, assuming monolayer deposition and 1:1 surface stoichiometry of Au on Pd. The molar ratio of the reducing agent to metal salt was initially selected at 1:10. Base on 1 g of Pd/TiO_2 and 1 monolayer of Au were used in process; the composition of the catalyst will be as follows,

Reagent: - Pd/TiO_2 catalyst

- Potassium dicyanoaurate(I), 98% ($KAu(CN)_2$)

Molecular weight = 288.10 g/mol

- Hydrazine solution, 35 wt.% in H_2O (N_2H_4)

Molecular weight = 32.05 g/mol

For 100 mL of Au stock solution used 0.1 g of $KAu(CN)_2$, thus Au stock solution containing Au metal as follow :

$$\text{Weight of Au in 100 mL of solution} = \frac{\text{weight of } KAu(CN_2) \times \%\text{purity} \times \text{M.W. of Au}}{\text{M.W. of } KAu(CN_2)}$$

$$= \frac{0.1\ \text{g} \times 0.98 \times 196.97\ \text{g/mol}}{288.10\ \text{g/mol}} = 0.067\ \text{g}$$

In 1.29 g of Pd on TiO_2 has 37.86% of dispersion and 2.75×10^{19} surface Pd sites/g cat, thus 1 monolayer of Au on Pd required 2.75×10^{19} Au sites, which calculation of volume Au solution required as follow :

$$\text{Solution of Au required} = \frac{\text{site of Au required} \times \text{M.W. of Au} \times \text{Con. of Au solution}}{\text{Avogadro's number}}$$

$$= \frac{2.75 \times 10^{19}\ \text{site} \times 196.97\ \text{g/mol} \times \dfrac{100\ \text{mL}}{0.067\ \text{g}}}{6.02 \times 10^{23}\ \text{site/mol}}$$

$$= 13.45\ \text{mL}\ (0.009\ \text{g of Au},\ 4\times10^{-5}\ \text{mol of Au})$$

Volume of N_2H_4 required

$$= \text{mole ratio of } N_2H_4 \text{ to Au} \times \%\text{purity} \times \text{M.W. of } N_2H_4 \times \rho \text{ of } N_2H_4 \times \text{mole of Au required}$$

$$= \frac{10\ \text{mol of } N_2H_4}{1\ \text{mol of Au}} \times 0.35 \times 32.05\ \text{g/mol} \times 1.10\ \text{g/mol} \times 4 \times 10^{-5}\ \text{mol}$$

$$= 0.0045\ \text{mL}$$

Volume of DI-water required = total volume – Au solution - N_2H_4 solution

= 100 mL – 13.45 mL – 0.0045 mL

= 86.55 mL

For calculation of Cu electroless bath was prepared in a similar way.

3. Calculation of Au and Cu on Pd/TiO_2 by incipient wetness impregnation method.

The 1.28 wt.% Pd/TiO_2 catalyst from SEA was used for preparation of Au and Cu on Pd/TiO_2 by incipient wetness impregnation method. Based on 100 g of Au-Pd/TiO_2 or Cu-Pd/TiO_2 used; the composition of the catalyst will be as follows:

Reagent : - Pd/TiO_2 catalyst

- Gold(III) chloride trihydrate ($HAuCl_4 \cdot 3H_2O$)

Molecular weight = 393.83 g/mol

- Copper(II) nitrate trihydrate ($Cu(NO_3)_2 \cdot 3H_2O$)

Molecular weight = 241.60 g/mol

For Au-$Pd/TiO_2$100 g :

Au required = 0.75 g

Pd/TiO_2 catalyst = 100-0.75 = 99.25 g

For 1 g of catalyst :

Au required = 0.75/100 = 0.0075 g

Gold(III) chloride trihydrate dissolved de-ionized water

$$\text{Au content in stock solution} = \frac{\text{Weight of Au required} \times \text{M.W. of } HAuCl_4 \cdot 3H_2O}{\text{M.W. of Au}}$$

$$= \frac{0.0075\ \text{g} \times 393.83\ \text{g/mol}}{196.97\ \text{g/mol}} = 0.015\ \text{g}$$

The pore volume of the Pd/TiO_2 is 0.3 mL/g and The total volume of impregnation solution which must be is 0.3 mL for the requirement of incipient wetness impregnation method, de-ionized water is added until the total volume of solution is 0.3 mL.

For Cu-$Pd/TiO_2$100 g :

Cu required = 0.30 g

Pd/TiO_2 catalyst = 100-0.30 = 99.70 g

For 1 g of catalyst :

Au required = 0.30/100 = 0.0030 g

Gold(III) chloride trihydrate dissolved de-ionized water

$$\text{Cu content in stock solution} = \frac{\text{Weight of Cu required} \times \text{M.W. of } Cu(NO_3)_2 \cdot 3H_2O}{\text{M.W. of Cu}}$$

$$= \frac{0.0030\ \text{g} \times 241.60\ \text{g/mol}}{63.55\ \text{g/mol}} = 0.0114\ \text{g}$$

APPENDIX B
CACULATION OF THE CYRSTALLITE SIZE

The crystallite size was calculation form the half-height width of the diffraction peak of XRD pattern using the Sherrer equation.

From Sherrer equation :

$$D = \frac{K\lambda}{\beta \cos\theta}$$

Where D = Crystallite size, Å
K = crystallite-shape fator = 0.9
λ = X-ray wavelength, 1.5418 Å for CuK_α
θ = Observed peak angle, degree
β = X-ray diffraction broadening, radian

X-ray diffraction broadening (β) is the corrected of a powder diffraction free from all broadening due to the instrument. The α-alumina was used as standard sample to provide instrumental broadending data (see Figure B.1). The most common correction for the X-ray diffraction broadening (β) can be obtaained by using the Warren's formular.

Warren's formular :

$$\beta = \sqrt{B_M^2 - B_S^2}$$

Where B_M = The measured peak width in radians at half peak height
B_S = The corresponding width of the standard material

Example : Calculation of the crystallite size of α-alumina

The half-height width of peak = 0.58° (from the **Figure B.1**)

$$= \frac{2\pi \times 0.58}{360}$$

$$= 0.0101 \text{ radian } (B_M)$$

The corresponding half-height width of α-alumina peak (from the B_S) value at the 2θ of 25.18° in **Figure B.2** = 0.00383 radian

$$\beta = \sqrt{0.0101^2 - 0.00383^2}$$

$$= 0.00935 \text{ radian}$$

β = 0.00935 radian

2θ = 25.18°

θ = 12.59°

λ = 1.5418

$$\text{The crystallite size} = \frac{0.9 \times 1.5418 \text{ Å}}{0.00935 \text{ radian} \times \cos 12.7}$$

$$= 152.06 \text{ Å}$$

$$= 15.2 \text{ nm}$$

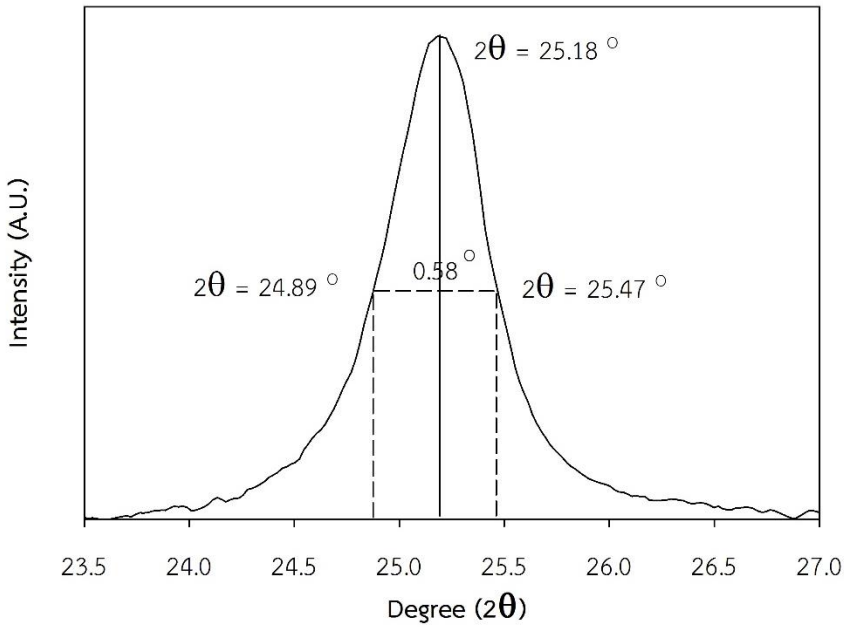

Figure B.1 The observation peak of α-alumina for calculating the crystallite size.

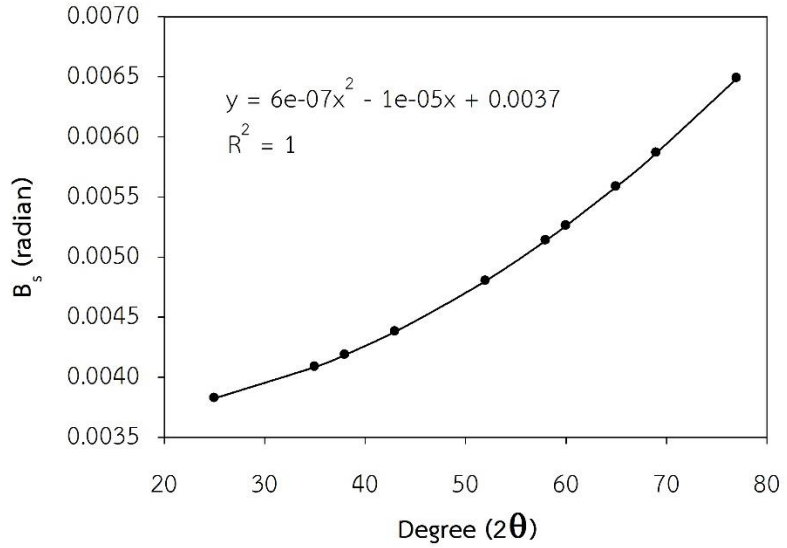

Figure B.2 The graph indicating that value of the line broadening attribute to the experimental equipment from the α-alumina standard.

APPENDIX C

CACULATION FOR METAL ACTIVE SITE AND DISPERSION

Hydrogen titration of O-precovered Pd was used for calculation Pd active sites and Pd dispersion by H_2 rapidly reacts with adsorbed O atoms to form H_2O and to cover the vacant Pd site with atomic H. For each Pd atom, 1.5 H_2 molecules are consumed.

$$\text{Metal dispersion} = 100 \times \frac{\text{molecules of Pd from } H_2 \text{ titration}}{\text{molecules of Pd loading}}$$

Volume H_2 titrated (V_{titra})

$$V_{titra} = \frac{V_{inj}}{m} \times \sum_{i=1}^{n} [1 - \frac{A_i}{A_f}]$$

V_{inj} = volume injected = 0.04 cm^3

m = mass of sample = 0.0514 g

A_f = area of peak last peak = 0.16776

Peak	A_i	A_i/A_f	$1-A_i/A_f$	V^i_{titra}
1	0.00138	0.008226	0.99177	0.77181
2	0.00222	0.013233	0.98677	0.76791
3	0.00961	0.057285	0.94272	0.73363
4	0.02701	0.161007	0.83899	0.65291
5	0.13522	0.806048	0.19395	0.15094
6	0.16776			
sum				3.0772

V_{titra} = 3.0772 cm^3/g

% Metal dispersion

$$\%D = S_f \times \frac{V_{titra}}{V_s} \times \frac{M.W.}{\%M} \times 100\% \times 100\%$$

S_f = stoichometer factor, Pd/H_2 = 2/3

V_{titra} = volume titrated = 3.0772 cm^3/g

V_s = molar volume of gas at STP = 22414 cm^3/mol

M.W. = molecular weight of the metal = 106.42 g/mol

%M = weight percent of the active metal= 1.29 %

$$\%D = \frac{2}{3} \times \frac{3.0772\ cm^3/g}{22414\ cm^3/mol} \times \frac{106.42\ g/mol}{1.29\%} \times 100\% \times 100\% = 37.86\%$$

Pd active sites

$$\text{Pd active sites} = S_f \times \frac{V_{titra}}{V_s} \times N_A$$

S_f = stoichiometry factor, Pd/H_2 = 2/3

V_{titra} = volume titrated = 3.0772 cm^3/g

V_s = molar volume of gas at STP = 22414 cm^3/mol

N_A = Avogadro's number = 6.02×10^{23} molecules/mol

Pd active sites =

$$\frac{2}{3} \times \frac{3.0772\ cm^3/g}{22414\ cm^3/mol} \times 6.02 \times 10^{23}\ molecules/mol$$

$$= 2.76 \times 10^{19}\ molecules/g$$

APPENDIX D

CACULATION FOR THE THEORETICAL COVERAGE AND ACTUAL COVERAGE

The theoretical coverage for second metal on Pd refers to monodisperse coverages of second metal/Pd at a 1:1 deposition stoichiometry. The actual coverage refer to the fraction of the Pd surface not coveraged by second metal for the bimetallic catalysts can be determined by subtracting their value from the total number of surface Pd sites for the monometallic Pd/TiO_2 catalyst.

Example : Calculation the theoretical coverage and actual coverage of 0.33%Au-Pd/TiO_2(ED) catalyst.

For 100 g of catalyst :

Au = 0.33 g

$$Pd = (100 - 0.33) \times \frac{1.29}{100} = 1.29 \text{ g}$$

Dispersion of Pd/TiO_2 = 37.9 %

$$\text{Total Pd site of } Pd/TiO_2 = \frac{1.29 \text{ g Pd}}{100 \text{ g cat}} \times \frac{6.02 \times 10^{23} \text{ molecules / mol}}{106.42 \text{ g / mol}}$$

$$= 7.30 \times 10^{19} \text{ molecules/g}$$

$$\text{Total Pd active site of monometallic catalyst} = 7.30 \times 10^{19} \times 0.379$$

$$= 2.76 \times 10^{19} \text{ molecules/g}$$

$$\text{Total sites of Au} = \frac{0.33 \text{ g of Au}}{196.97 \frac{\text{g}}{\text{mol}}} \times 6.02 \times 10^{23} \frac{\text{molecules}}{\text{mol}}$$

$$= \frac{1.01 \times 10^{21} \text{ molecules of Au}}{100 \text{ g of catalyst}}$$

$$= 1.01 \times 10^{19} \text{ molecules of Au/ g of catalyst}$$

$$\text{The theoretical coverage} = \frac{\text{Total sites of Au}}{\text{Total Pd active site of monometallic catalyst}}$$

$$= \frac{1.01 \times 10^{19}}{2.76 \times 10^{19}} = 0.37$$

The actual coverage =

$$\frac{\text{Total Pd active sites of monometallic catalyst - Pd active sites not coverage of Au}}{\text{Total Pd active sites of monometallic catalyst}}$$

Dispersion of 0.33%Au-Pd/TiO_2 = 32.2 %

Total Pd active site of bimetallic catalyst = $7.30 \times 10^{19} \times \frac{32.2}{100} = 2.35 \times 10^{19}$ molecules/g

$$\text{The actual coverage} = \frac{2.76 \times 10^{19} - 2.35 \times 10^{19}}{2.76 \times 10^{19}} = 0.15$$

APPENDIX E

CACULATION OF GAS HOURLY SPACE VELOCITY (GHSV)

Calculation of Gas Hourly Space Velocity (GHSV)

$$\text{GHSV } (h^{-1}) = \frac{\text{Flow rate}}{\text{Volume of catalyst}}$$

Volume of catalyst

Diameter of reactor (d) = 10 mm

High of catalyst (h) = 3 mm

$$\text{Volume} = \frac{\pi d^2 h}{4}$$

$$= \frac{3.14 \times 10^2 \times 3}{4}$$

$$= 235.5 \text{ mm}^2$$

Flow rate

$$\frac{10 \text{ cm}^3}{60 \text{ s}} = \frac{10 \times 10 \times 10 \times 10 \times 3600}{60}$$

$$= 600{,}000 \text{ mm}^3/\text{h}$$

Gas Hourly Space Velocity (GHSV)

$$\text{GHSV } (h^{-1}) = \frac{600{,}000}{235.5} \ h^{-1}$$

$$= 2548 \ h^{-1}$$

APPENDIX F

CACULATION CURVE

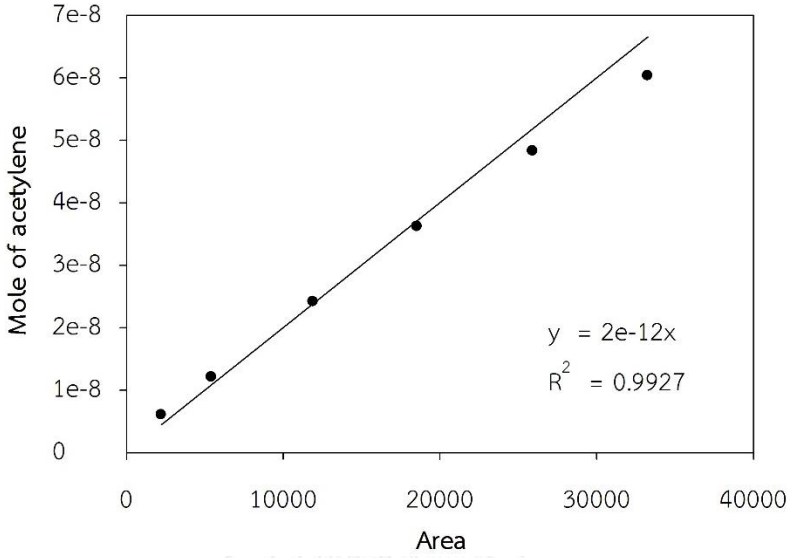

Figure E.1 The calibration curve of acetylene from GC-8APF (FID)

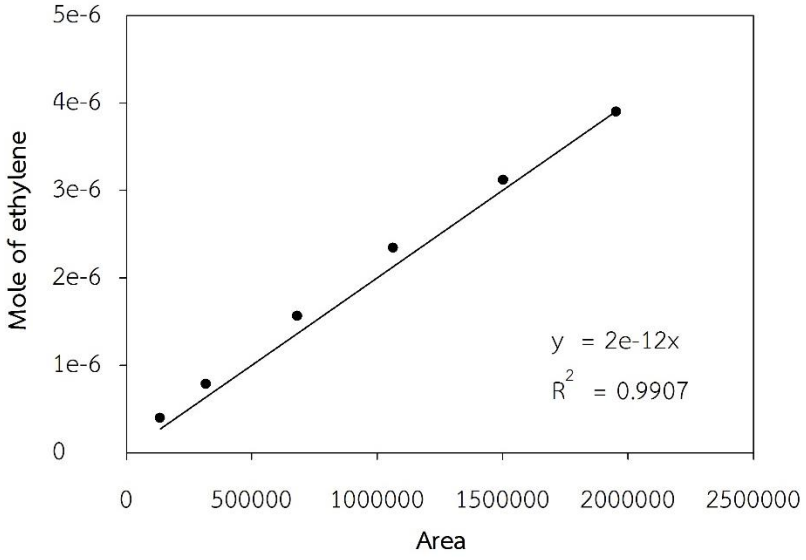

Figure E.2 The calibration curve of ethylene from GC-8APF (FID)

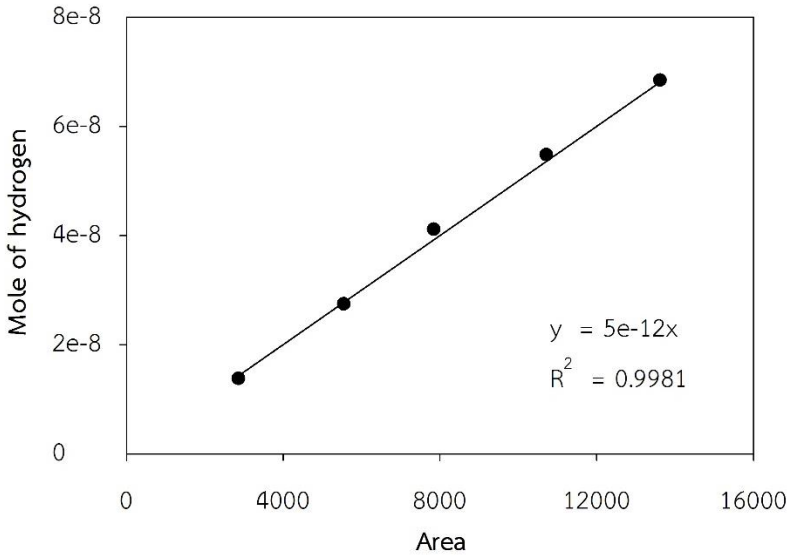

Figure E.3 The calibration curve of hydrogen from GC-8APT (TCD)

APPENDIX G

CACULATION OF C_2H_2 CONVERSION AND C_2H_4 SELECTIVITY

The catalytic performance for selective hydrogenation of acetylene was evaluated in terms of activity for acetylene conversion and ethylene selectivity based on the following equation :

$$C_2H_2 + H_2 \longrightarrow C_2H_4$$

$$C_2H_4 + H_2 \longrightarrow C_2H_6$$

Acetylene conversion was calculated from moles of acetylene converted with respect to acetylene if the feed:

$$\text{Acetylene conversion (\%)} = \frac{\text{mole of } C_2H_2 \text{ in feed - mole of } C_2H_2 \text{ of product}}{\text{mole of } C_2H_2 \text{ in feed}} \times 100$$

Where mole of acetylene can be measured from the calibration curve of acetylene in **Figure E.1** APPENDIX E.

Mole of C_2H_2 = (area of C_2H_2 peak from integrator plot of GC-8APT) $\times 2\times10^{-12}$

Ethylene selectivity was calculated from moles of H_2 and C_2H_2:

$$\text{Ethylene selectivity (\%)} = \frac{dC_2H_2 - (dH_2 - dC_2H_2)}{dC_2H_2} \times 100$$

Where dC_2H_2 = mole of C_2H_2 in feed - mole of C_2H_2 in product

dH_2 = mole of H_2 in feed - mole of H_2 in product

mole of H_2 can be measured employing the calibration curve of H_2 in **Figure E.3** APPENDIX E.

Mole of H_2 = (area of H_2 peak from integrator plot of GC-8APT) $\times 5\times10^{-12}$

VITA

Miss Nisarat Wimonsupakit was born on September 26th, 1992 in Chachoengsao, Thailand. She received the Bachelor's Degree in Chemical Engineering from Department of Chemical Engineering, Faculty of Engineering and Industrial Technology, Silpakorn University, Nakhonpathom, Thailand in May 2014. Thereafter, she entered to study in Master's Degree of Chemical Engineering at Department of Chemical Engineering, Chulalongkorn University, Bankok Thailand since 2014 and joined center of excellence on catalysis and catalytic reaction engineering research group.